Long-term phenotypic effects following vitrified-thawed embryo transfer in a rabbit model

Ximo Garcia-Dominguez[1+], David. S. Peñaranda[1+], Guillem Estruch[2], José Blanca[3], Victor García-Carpintero[3], Joaquín Cañizares[3], Francisco Marco-Jiménez[1], José Salvador Vicente[1*]

1Laboratory of Biotechnology of Reproduction, Institute for Animal Science and Technology (ICTA), Universitat Politècnica de València, 46022 Valencia, Spain.

2Aquaculture and Biodiversity Research Group. Institute for Animal Science and Technology (ICTA), Universitat Politècnica de València, 46022 Valencia, Spain.

3Institute for the Conservation and Breeding of Agricultural Biodiversity (COMAV-UPV), Universitat Politècnica de València, 46022 Valencia, Spain.

+ These authors contributed equally to this work

* Corresponding author

E-mail: jvicent@dca.upv.es (JSV)

Abstract

Since the first human was conceived through in vitro fertilisation in 1978, over 6.5 million babies have been born by assisted reproductive technologies (ARTs). Although most ART babies and children seem healthy, in recent years several studies have evidenced a potential impact of ARTs on long-term development and health. Herein, we have developed an animal model to determine whether vitrified embryo transfer procedure induces phenotypic changes over the growth performance and in the complementary transcriptomic and proteomic analyses at hepatic level. To this end, 2 populations were developed; vitrified embryos transferred to the surrogate mothers (VT) and naturally conceived animals (NC). After delivery, animals were weighed weekly from 1 to 20 weeks of age. In adulthood, animals were euthanized and organs were harvested and weighed. After that, liver tissue was used to identify changes in the transcriptomic and proteomic profile. At adulthood, VT group showed significant lower body, liver and heart weight. After functional analysis of RNA-Seq data, a subset of 96 differentially expressed transcripts in VT animal were related to alteration in zinc homeostasis, lipid metabolism, and hepatic immune pathways. After proteomic analysis, a subset of 76 differentially expressed proteins also revealed some disturbed metabolic pathways related with the lipid and glycan metabolism, and an impaired oxidative metabolism related to ATP synthesis in the mitochondria. Current findings suggest that progeny derived after transfer of vitrified embryos have long-term consequences on growth rate and vital organs weights in adulthood, correlated with molecular signatures at transcriptomic and proteomic level of hepatic tissue.

Keywords: Rabbit, vitrification, impact, transcriptome, proteome

Introduction

Since the first human conceived through *in vitro* fertilisation in 1978, it has been estimated that more than 6.5 million babies born by assisted reproductive technologies (ARTs, [1]). Nevertheless, from the beginning of the application of ARTs, there has been concern about the influence of these technologies on development, and in consequence several epidemiological studies have reported on this issue, associating ARTs with low birth weight, preterm birth, heart disease, hypertension, hyperlipidaemia, insulin resistance and increased risk of type 2 diabetes or adverse neurodevelopmental outcome [1-5]. However, it is difficult to determine in humans whether these effects are really caused by ARTs per se or originate from either genetic abnormalities or risk factors intrinsic to infertile patients [4]. Based on animal models that avoid these confounding factors, analogous effects have been reported, evidencing long-lasting consequences of ARTs such as glucose intolerance, insulin resistance, cardiometabolic disorders, hypertension, behavioural deficits, memory loss, abnormal hepatic and fat metabolomes, placenta dysfunction, body weight and organ weight changes, altered locomotion and shorter lifespan [6-19]. Till now, the vast majority of fertility researchers have been trying to improve the success of ARTs based on apparently healthy babies at home, but only a few are trying to discern whether ARTs leaves a subtle legacy in offspring [20].

In recent years, there has been an increasing trend towards ART cycles that include a cryopreservation procedure that maximises the efficacy of ovarian stimulation cycles in an IVF treatment by allowing storage of the excess embryos and their later use, but also to enable fertility preservation [21, 22]. Hence, cryopreservation of human embryos is currently more important than ever for the cumulative pregnancy rate after IVF [21]. The cryopreservation is a technique in which gametes and embryos are exposed to cryoprotectant solutions and are stored at sub-zero temperatures until needed for use. Although no studies have evidenced genotoxic or teratogenic effects [23], cryopreservation is known to cause extensive damage with marked deleterious effect on embryonic health, compromising its full-term development due to the associated higher rate of pregnancy complications [24, 25]. In addition, offspring present higher risk of high birth weight, high prenatal growth rate (large for gestational age) and hypertensive disorders [26].

Recently, studies carried out under several omics approaches have reported an increased incidence of metabolic activity disorders, cellular stress and changes in developmental potency that varied depending on the in vitro manipulation conditions [27-32]. ART related disorders in mice and rabbit have been evidenced at placental function level by transcriptomic and proteomic studies [17, 33-35]. Furthermore, disturbances in the protein profile of umbilical veins and foetuses derived from ART have been identified, suggesting molecular disorders that can affect later life stages [36, 37]. It has been demonstrated that in vitro manipulation incurs in molecular anomalies beyond parturition, which have been associated with liver weight changes [7], increased fat deposition [16], lower pancreatic

weight and impaired functionality [13], endothelial dysfunction, increased stiffness of the vasculature and arterial hypertension [12], heart physiology [38] and functionality [13], behavioural and anxiety level changes [7, 39], muscle physiology [16] and cardiometabolic profile [40]. However, there is a lack of knowledge and understanding around the role of vitrified embryo transfer procedure in adulthood.

To address this issue, we have developed a rabbit model to study the effects of vitrified embryo transfer procedure on body growth and organs weight in adulthood, and hepatic tissue on a global scale in terms of molecular signatures at transcriptomic and proteomic level.

Materials and Methods

All chemicals, unless otherwise stated, were reagent-grade and purchased from Sigma-Aldrich Química S.A. (Alcobendas, Madrid, Spain). All the experimental procedures used in this study were performed in accordance with Directive 2010/63/EU EEC for animal experiments and reviewed and approved by the Ethical Committee for Experimentation with Animals of the Universitat Politècnica de València, Spain (research code: 2015/VSC/PEA/00061).

Animals

Healthy animals used as control (naturally conceived animals), embryo donors and surrogate mothers (vitrified and transferred animals) belonged to the

117 synthetic strains selected by Instituto de Ciencia y Tecnología Animal at the
118 Universitat Politècnica de València since the 80s.
119

120 Experimental Design

121 Figure 1 illustrates the experimental design. Initially, 2 experimental populations
122 were developed: one from vitrified embryos transferred to the surrogate mothers
123 (VT) and other from naturally conceived animals (NC). In both experimental
124 groups, females were artificially inseminated (AI) with semen of unrelated males
125 from the same strain. In the VT group, 3 days after AI, the embryos were
126 recovered, vitrified and then transferred to surrogate mothers by laparoscopy.
127 Meanwhile, NC offspring were generated letting the females give birth after AI.
128 After delivery, male offspring were weighed every week until adulthood. At 56
129 weeks of age, animals were euthanised and organs were weighed. From the liver,
130 6 individual biopsies were obtained (3 VT and 3 NC). Over the same samples,
131 complementary RNA sequencing and proteomic studies were performed.
132
133

134 In vivo embryo production and collection

135

136 A total of 28 donors were AI with semen from mature tested males. When the AI
137 was performed, females were injected with 1 µg of buserelin acetate to induce
138 ovulation. Then, donors were euthanised 72 h post-AI and embryos were
139 recovered. Briefly, the reproductive tract was retrieved and each oviduct and
140 uterine horn (the first one third) was perfused with 5 ml of embryo recovery media,

consisting of pre-warmed solution (≈20-25 ºC) of Dulbecco's Phosphate-Buffered Saline (DPBS) solution supplemented with $CaCl_2$ (0.132 g/L), 0.2% (w/v) of bovine serum albumin (BSA) and antibiotics (penicillin 100 IU/mL, streptomycin 100 µg/mL and amphotericin B 0.25 µg/mL). After recovery, morphologically normal embryos (correct developmental stage, homogenous blastomeres and intact spherical mucin coat and zona pellucida) were selected and vitrified. A total of 301 embryos were vitrified.

Vitrification and warming procedure

Embryos were vitrified and warmed using the methodology described by Vicente et al. [41]. Embryos were vitrified in two-step addition procedure at room temperature (≈20-25 ºC). In the first step, embryos were placed for 2 min in a solution consisting of 10% (v/v) dimethyl sulphoxide (DMSO) and 10% (v/v) ethylene glycol (EG) in DPBS supplemented with 0.2% of BSA. In the second step, embryos were suspended for 30 s in a solution of 20% DMSO and 20% EG in DPBS supplemented with 0.2% of BSA. Then, embryos suspended in vitrification medium were loaded into 0.125 mL plastic straws (French ministraw, IMV, L'Aigle, France) adding 2 sections of DPBS at either end of each straw, separated by air bubbles. Finally, straws were sealed and plunged directly into liquid nitrogen. Warming was done by horizontally placing the straw 10 cm from liquid nitrogen for 20-30 s and when the crystallisation process began, the straws were immersed in a water bath at 20ºC for 10-15 s. The vitrification medium was removed rinsing the embryos into a solution containing DPBS with 0.33 M sucrose for 5 min, followed by one bath in a solution of DPBS for another 5 min.

166 Only non-damaged embryos (intact mucin coat and pellucid zone) were
167 considered to continue with the transfer. From the 301 vitrified embryos, 287 were
168 recovered successfully and 272 (non-damaged embryos) were catalogued as
169 transferable attending to International Embryo Transfer Society classification.
170

171 ## Embryo transfer

172

173 Embryos were transferred into the oviducts of 26 surrogate mothers by
174 laparoscopy, following the procedure previously described by Besenfelder and
175 Brem, [42]. The mean number of transferred embryos per surrogate mothers was
176 10.5 (ranged from 6 to 19). Briefly, ovulation was induced in the surrogate
177 mothers with an intramuscular dose of 1 µg Buserelin Acetate 68–72 h before
178 transfer. During laparoscopy, surrogate mothers were anaesthetised by an
179 intramuscular injection of xylazine (5 mg/Kg; Bayer AG) followed by an
180 intravenous injection of ketamine hydrochloride (35 mg/Kg; Imalgene, Merial SA,
181 Lyon, France) 5 min later. During laparoscopy, one dose of morphine
182 hydrochloride (3 mg/Kg; Morfina, B. Braun, Barcelona, Spain) was administered
183 intramuscularly. After surgery, animals were treated with antibiotics (4 mg/Kg of
184 gentamycin each 24 h) and analgesics (0.03 mg/kg of buprenorphine
185 hydrochloride each 12 h and 0.2 mg/kg of meloxicam every 24 h; Alvet Escarti
186 S.L. Guadassuar, Spain) for 3 days.
187

188

189 ## Control progeny

The control progeny (NC) group were obtained following the common management of rabbit reproduction without embryo vitrification or embryo transfer procedures. Briefly, contemporaneous control offspring were produced using artificial insemination as a reproduction technique. This procedure was carried out using 0.5 mL of diluted fresh semen from fertile males. Immediately after that, ovulation was induced in inseminated females by an intramuscular injection of 1 µg of buserelin acetate.

Body growth, organs weight and peripheral blood parameters study

A total of 65 males were weighed weekly from 1 to 20 weeks of age (30 from VT and 35 from NC groups). Then, body growth was estimated by nonlinear regression using the Gompertz curve equation, well suited for rabbits [43]: $y= a \exp[-b \exp(-kt)]$, where y is the observed body weight of one individual at a specific age (t). The rest of the parameters (a, b and k) of the Gompertz function have a biological interpretation: a can be interpreted as the mature body weight (BW), maintained independently of short-term fluctuations; b is a timescale parameter related to the initial body weight; k is a parameter related to the rate of maturing (growth rate). Furthermore, BW differences between the experimental groups were evaluated weekly. In addition, males were euthanised at week 56 (late adulthood), when the growth plate is closed [44] determining the

213 body weight and vital organs (liver, lungs, heart, kidneys and adrenal glands),
214 spleen and gonads weight.
215
216 Prior to euthanasia, individual blood samples were obtained and dispensed into
217 a EDTA-coated tube (Deltalab S.L., Barcelona, Spain). Within 10 minutes of
218 collection, samples were analysed using an automated veterinary haematology
219 analyser MS 4e automated cell counter (MeletSchloesing Laboratories, France)
220 according to the manufacturer's instructions. The blood parameters recorded
221 were: white blood cells, lymphocytes, monocytes, granulocytes, red blood cells
222 and haematocrit. Samples were processed in duplicate.
223
224 A general linear model (GLM) was fitted for the analysis of BW in each week,
225 including as fixed effect the experimental group with 2 levels (VT and NC) and
226 the covariate number of liveborn at birth. Differences in BW in each week
227 between the experimental groups were computed and plotted as the difference
228 in their least squares means ± standard error of means (NC-VT). As previously,
229 for organ weight and blood parameters analysis a GLM was fitted including as
230 fixed effect the experimental group (VT and NC), but in the case of organ weights
231 data were corrected using BW as covariate.
232
233 Growth curves for male rabbits were fitted following the Gompertz model as
234 described by Laird [45], as the Gompertz curve is appropriate to describe rabbit
235 growth [43]. The parameters of the Gompertz curve were estimated and
236 differences between experimental groups for the Gompertz curve parameters
237 were tested using GLM as previously. Differences of $p<0.05$ were considered

238 significant. Statistical analyses were performed with SPSS 21.0 software
239 package.
240

241 Sampling for the molecular signature of hepatic tissue

242

243 A total of 6 samples (3 VT and 3 NC) were generated obtaining some liver
244 biopsies randomly. The samples were immediately washed with DPBS to remove
245 blood remnants. After that, one part from each sample was stored in RNA-later
246 (Ambion Inc., Huntingdon, UK) at -20 ºC for transcriptomic analysis, while the
247 other part was directly flash frozen in liquid nitrogen and stored at -80º C for the
248 proteomic study. Then, all samples were derived from the same animal cohorts.
249
250

251 Transcriptome: RNA isolation, RNA-Seq and functional
252 analysis

253

254

255 Samples were shipped to the Macrogen company (Seoul, South Korea).
256 Afterwards, the mRNA purification was carried out using Sera-mag Magnetic
257 Oligo (dT) Beads, followed by buffer fragmentation. Reverse transcription was
258 followed by PCR amplification to prepare the samples to be sequenced, keeping
259 the strand information, in an Illumina Hiseq-4000[D1] sequencer (Illumina, San
260 Diego, USA). Resulting raw sequences are available at the NCBI Sequence Read
261 Archive (BioProject ID: PRJNA483095, Supplemental Table 1). Raw read

qualities were assessed using FastQC software [46]. Reads were mapped keeping strandness information against the reference genome for *Oryctolagus cuniculus*, version 2.0 from Ensembl using hisat2 [47]. Expression was counted using stringtie [48]. This counting was guided using the genome annotation and a unified set of transcripts was created for the samples analysed. Then, a Fragments Per Kilobase of transcript per Million (FPKM) table with gene expression for each sample was generated and used for assess the expression profiles of each sample by PCA. Then, a table with raw counts were generated. This table was used for the differential expression analyses using edgeR [49] integrated in the webservice platform WebMeV [50]. Only differential expressed genes (DEG) with a threshold of a false discovery rate (FDR) of < 0.05 were considered for further analyses.

For comparison between groups, further filtering of DEGs was made. Only genes with an absolute value of log2 fold change => 1.2 and at least one of the samples involved in the comparison with a Transcripts Per Kilobase Million (TPM) of 1 were kept. Then, in those samples which registered a coefficient of variation higher than 50% and a difference between mean and median higher than 1, the gene was maintained if half of the samples of the most expressed condition group had an expression two times higher than the mean of the other group.

ClustVis software was used to perform the Principal Component Analysis (PCA) of all expression data and the Heat-Map clustering [51]. Functional annotation of DETs, enrichment analysis of their associated GO terms and KEGG pathways

286 analysis were computed using the Bioinformatic software: David Functional
287 Annotation Tool (version 6.8; October 2016), considering a P-value < 0.05.
288

289 Proteome: Protein extraction, identification and
290 functional analysis

291

292 Here we maintained the same cohort of animals used for the transcriptomic study.
293 Samples were placed in 8M urea (Malinckrodt AR®, LabGuard®) in
294 homogenisation tubes (^{RT}Precellys® Ceramic Bead Tube) and then ground using
295 the homogeniser PrecellysTM Control Device (Bertin Technologies). Tissue
296 extracts were subjected to cold acetone precipitation and pellets were
297 resuspended in 8M urea, determining the protein concentration by the BCA assay
298 kit (ThermoScientific, Meridian Rd., Rockford, IL, USA). A volume of sample with
299 a protein amount of 50 µg was processed. Briefly, samples were subjected to
300 denaturation, reduction and alkylation prior to the digestion step with
301 trypsin/Lysine-C enzyme mix (Trypsin/Lys-C mix mass spec grade, Promega).
302 Digested peptides were purified using C18 columns (MicroSpin Column 96/pk,
303 C18 Silica, 5-200 µL loading, 5-60 µg capacity, The Nest Group, Inc.) and
304 samples were dried and stored at -20 ºC. Then, the resulting pellets were
305 analysed using a Dionex UltiMate 3000 RSLC Nano System coupled to the Q
306 Exactive™ HF Hybrid Quadrupole-Orbitrap Mass Spectrometer (Thermo
307 Scientific, Waltham, MA, USA) as described in [52].
308

309 The peptide masses were searched against a protein database for the taxa
310 *Oryctolagus cuniculus* (UniProt) using the freely available MaxQuant software

311 package (version 1.5.5.1, Max Planck Institute of Biochemistry), with first search
312 peptide tolerance of 20 ppm, main search peptide tolerance of 4.5 ppm, 1% false
313 discovery rate (FDR), trypsin and lysC digestion and carbamidomethyl cysteine
314 as fixed modification, and oxidised methionine as variable modification. Match
315 between runs was considered (Match time window of 1 min and an Alignment
316 Time Window of 20 min). Label-free quantification (LFQ) was used to obtain the
317 normalised LFQ intensity. Contaminants and reverse proteins were removed
318 from the analysis. Only proteins with at least 2 MS/MS counts were considered.
319
320 InfernoRDN application (Pacific Northwest National Laboratory), which provides
321 an easy-to-use R (version 3.3.1) for proteomic data analysis, was used to analyse
322 and compare the intensity and the LFQ intensity data, including Log2
323 transformation and Analysis of Variance (ANOVA). Only proteins that displayed
324 values of intensity≠0 in the 2 control samples and at least 3 vitrified samples were
325 included in the ANOVA. After the InfernoRDN analysis, proteins with ANOVA p-
326 value<0.05 were subjected to cross comparison between groups (control vs
327 vitrified). Proteins with an average fold change (FC)≥2 or ≤0.5, or with a t-
328 test<0.05 (and a FC ≥1.5 or ≤0.66), were selected for the subsequent functional
329 annotation.
330
331 ClustVis software was used to perform the Principal Component Analysis (PCA)
332 of all expression data and the Heat-Map clustering [51]. Functional annotation of
333 differentially expressed proteins (DEPs), enrichment analysis of their associated
334 GO terms and the KEGG pathways analysis were computed using the

335 Bioinformatic software: David Functional Annotation Tool (version 6.8; October
336 2016), considering a P-value < 0.05.

337

338 Results

339

340 Males derived after vitrified embryo transfer procedure
341 exhibit lower growth performance and lower body and
342 organ weights in adulthood

343

344 Although at parturition the VT group showed higher individual weight than NC
345 group (67.8±1.46 vs 60.5±1.72 g, p<0.05), even after data were corrected by
346 number of born offspring (6.9±0.38, significant covariate effect at p<0.05), a
347 reduced growth was observed from the second week of life until adulthood was
348 reached (Figure 2 and Figure 3). Hence, the parameters governing the Gompertz
349 growth curve (Figure 2) revealed that its estimated values; related with the initial
350 body weight condition (b parameter: 4.55 ± 0.124 vs 5.23 ± 0.209, p<0.05),
351 growth velocity (k parameter: 0.16 ± 0.005 vs 0.20 ± 0.007, p<0.05) and mature
352 body weight (a parameter, 4873.2 ± 82.32 vs 5275.5 ± 105.20, p<0.05) were
353 lower in the VT vs NC group, respectively. After weaning (from 4 to 9 weeks of
354 age), mean weight differences between groups were 248.0±20.98 g (NC-VT ±
355 standard error, p<0.05, Figure 3). From this age, the weight differences were still
356 increased until adulthood (from 10 to 56 weeks of age), the mean weight

differences between groups being 696.8±44.42 g (NC-VT ± standard error, $p<0.05$, Figure 3).

At 56 weeks of age, VT group showed lower body weight (5.3 ± 0.11 vs 5.7 ± 0.10 Kg, for VT vs NC group respectively, $p<0.05$, Table 1). Moreover, VT group showed lower liver (92.8 ± 2.37 vs 102.1 ± 2.51 g [10.0%], for VT vs NC group respectively, $p<0.05$) and heart weight (11.6 ± 0.44 vs 13.1 ± 0.43 g [12.9%], for VT vs NC group respectively, $p<0.05$), even after data were corrected by body weight (Table 1). No significant weight differences were observed for the rest of the organs analysed.

Vitrified embryo transfer procedure seems to be neutral on the peripheral blood parameters

As shown in Table 2, there were no significant differences in peripheral profile of blood cells (white blood cells, red blood cells, and haematocrit), between VT and NC groups.

The liver transcriptome was influenced by vitrified embryo transfer procedure

The transcriptomes from adulthood liver tissue from VT were compared with NC counterparts. The mean number of raw reads was 48.62 ± 4.48 (±SD) millions, and transcripts from 13.908 to 14.524 different genes (from a total of 24.964

382 annotated transcripts of Orycun2.0) were detected in each individual. Principal
383 Component Analysis (PCA) and Heat-Map analysis showed that, while the NC
384 samples showed higher variability, the VT samples clustered together (Figure 4A,
385 4B). RNA-Seq data analysis identified 133 differentially expressed transcripts
386 (DETs) between the VT and NC groups. Of the transcripts that were significantly
387 different, a total of 96 DETs were recognised by the DAVID bioinformatics tool.
388 From these DETs, there was a higher number of downregulated (68/96, [70.8%])
389 than up-regulated (28/96, [29.2%]) in VT samples compared with NC group. A
390 description of DETs and the fold change values obtained are shown in Table 3.
391 Functional GO term enrichment and KEGG pathway analysis of DETs were
392 recorded in Table 4. This analysis suggests transcriptomic alteration related to
393 zinc homeostasis, lipid metabolism and hepatic immune pathways in VT group
394 animals.
395

396 The liver protein profile was influenced by vitrified
397 embryo transfer procedure

398

399

400 In this case, the protein profiles of adulthood liver tissue from VT were compared
401 with NC counterparts. Mean number of MS/MS spectra per sample submitted for
402 the MaxQuant analysis was 76408 ± 950 (±SD). The number of peptides
403 identified ranged from 10708 to 12059 and the number of proteins from 1707 to
404 1782 (from a total of 22929 proteins included in Oryctolagus cuniculus database
405 [Uniprot]) was detected in each individual. PCA and Heat-Map analysis showed

406 that, despite expected individual variability, samples from each group were
407 clustered together (Figure 4C, 4D). Protein data analysis identified 90 DEPs in
408 VT animals compared with NC group. Of the proteins that were significantly
409 different, a total of 76 DEPs were recognised by the DAVID software. From these
410 DEPs, there was a higher number of downregulated (60/76, [78.9%]) than up-
411 regulated (16/76, [21.1%]). Annotation of DEPs and the fold change values
412 obtained are shown in Table 5. Functional GO term enrichment and KEGG
413 pathway analysis of DEPs were recorded in Table 6. This analysis suggests an
414 impaired oxidative metabolism related to ATP synthesis in the mitochondria in VT
415 group animals.
416
417

418 Discussion

419

420 The progress made by ART during the past 2 decades makes a future without
421 their use inconceivable [53]. However, it is well established that the use of these
422 technologies has consequences on development and modification of the embryo
423 epigenome [7, 53-56]. Hence, and in line with our previous studies, we again
424 corroborate that male progeny born after transfer of vitrified embryos result in a
425 reduced growth rate and vital organs weights in adulthood [34, 57]. In addition,
426 multi-omics analyses of hepatic tissue revealed modifications in lipid metabolism
427 and energy metabolism that could be implicated in growth and body weight.
428 Importantly, in our study, there is strong evidence that vitrified embryo transfer
429 manipulation technique represent a clear example of the active phenotypic

plasticity exhibited by the embryo, where irreversible phenotypic variation in traits of individuals induce modifications of development and growth [58].

Today, cryopreservation is an essential component in the treatment of patients undergoing ART [59, 60]. The choice of a cryopreserved cycle avoids the suboptimal endometrium generated by supra-physiologic hormonal levels during a conventional ovarian stimulation [61, 62], improving the implantation and pregnancy rates and reducing the risk of preterm birth [63, 64]. However, although cryopreservation was considered a neutral technique for years [65, 66], some recent studies have revealed potential adverse effects throughout gestation [24, 25, 67, 68]. Associations between ART and birth defects or stillbirth are controversial, but the vast majority of studies indicated that the increased risk of birth defects are attributed to maternal characteristics related to infertility [69-72]. However, in recent years, research studies are starting to learn about the long-term health of people conceived after ART treatment, but there are only few longitudinal studies about the effect of embryo cryopreservation on health risks [73-75]. To test the effect of embryo vitrification in adulthood, we used an animal model to minimise external confounding factors. It is important to state that, in our study, the offspring born after transfer of vitrified embryos were apparently healthy, which was also corroborated in adulthood by outcomes of peripheral blood features. The most remarkable finding regarding to long-term consequences of vitrification at late adulthood was lower growth, decreased body weight and a lower weight of some vital organs, such as the liver and heart. Even though higher body weight was observed at parturition, from the third-fourth week of age till adulthood animals born after transfer of vitrified embryos showed a

455 reduced body growth curve, although in rabbit these deviations can be restored
456 at adulthood through compensatory growth [76]. Studies on health outcomes of
457 offspring conceived by ART in animals [77] and human [78, 79] also revealed a
458 significant increase in the birth weight. This may be related to the fact that
459 embryos are grown for one extra day *in vitro* after thawing to compensate for the
460 loss of cells in the freezing and thawing processes [79]. Imprinting modifications
461 of some growth-related genes have also been suggested to explain the
462 phenotype variations observed in animals obtained after embryo
463 cryopreservation [57,79]. Supporting this, previous studies have also reported
464 variations in body weight after embryo cryopreservation [23, 57, 80], as well as
465 after *in* vitro culture and transfer [81]. From these studies, we can learn that
466 different ARTs protocols would lead to different outcomes via specific epigenetic
467 modifications. Collectively, these findings suggest that features exhibited vitrified
468 embryo transfer manipulation technique seems to be a clear manifestation of the
469 embryonic active phenotypic plasticity, which refers to the capacity of a genotype
470 to produce different phenotypes in response to environmental variation,
471 contributing to diversity among individuals, populations and species [58].
472
473 Today, the 'omics' sciences are used to describe the flow of biological information
474 in an organism [82]. Based on the phenotyped changes observed in adulthood of
475 animals born after transfer of vitrified embryos, we assessed the molecular
476 signatures at hepatic level in order to find out the possible vitrification effects on
477 both transcriptome and proteome profile "what appears to be happening"
478 (transcriptome) and "what makes it happen" (proteome). In our study, we
479 registered significant differences in both levels, 133 genes and 90 proteins.

480 Furthermore, the PCA revealed that animals born after transfer of vitrified
481 embryos and animals born after natural conception formed a distant cluster. The
482 overall result suggests that vitrification could alter hepatic function, impairing the
483 correct establishment of the “growth hormone/insulin-like growth factor type I”
484 axis whose perturbations are responsible for many important complications, such
485 as growth disturbance [83-85]. Among the differential transcripts, we detected 3
486 metallothioneins (metallothionein-1A, metallothionein-2A and metallothionein-
487 2D) involved in multiple interconnected signalling pathways related to “negative
488 regulation of growth” and “cellular response to zinc ion” GO terms.
489 Metallothioneins (MT) are small molecular weight and cysteine-rich proteins that
490 play many important biological roles, including zinc (Zn) trafficking and potential
491 protective effects against oxidative stress and toxic metals [86-87]. Liver is the
492 primary storage organ of Zn, is sensitive to Zn deficiency, and is the most
493 responsive organ for antioxidative function [88]. Zn plays a key role in growth via
494 protein synthesis and antioxidant defence, and Zn deficiency causes growth
495 deficits [89-90]. In concordance, previous studies have also suggested that
496 improved growth performance may result from the role of Zn as a crucial
497 component in the systemic antioxidative and immune network [91]. Nonetheless,
498 KEGG analysis reveals a disturbed “mineral absorption” associated with Zn due
499 to downregulation of MT coding genes after transfer of vitrified embryos,
500 suggesting an impaired Zn homeostasis that can incur in the lower growth
501 exhibited by the vitrified progeny. Similar positive correlation between Zn
502 availability and MT expression with the growth performance has been described
503 in farm animals and children [89, 92, 93]. As regards molecular function, DETs
504 were highlighting the “oxidoreductase activity, acting on paired donors, with

505 oxidation of a pair of donors resulting in the reduction of molecular oxygen to 2
506 molecules of water" terms, which are hierarchical and associated with desaturase
507 enzyme activity. Desaturase and elongase enzymes play a crucial role in the
508 metabolism regulation and biosynthesis of unsaturated fatty acids [94-96]. We
509 observed that 2 desaturases and 1 elongase were becoming downregulated in
510 hepatic tissue in animals obtained after transfer of vitrified embryos. Interestingly,
511 Zn also acts as a cofactor of the fatty acids desaturase enzymes, whose
512 metabolic roles are required for optimal growth, immune response, gene
513 expression, visual development, neurotransmission and cognition [95, 97]. So,
514 as expected, these findings were in concordance with the perturbed "biosynthesis
515 of unsaturated fatty acids" and "fatty acid metabolism" highlighted by the KEGG
516 pathways analysis, which supported a disturbed lipid metabolism in hepatic tissue
517 due to impaired Zn metabolism after embryo vitrification. A recent report has
518 demonstrated that ART induces modifications in the lipid metabolism in foetal
519 hepatic tissue [18], which could be maintained in later life stages [18, 98-100],
520 and even into adult life as our results suggest.
521
522 The most significantly increased transcript in VT animals was the peptidoglycan
523 recognition protein 2 (*PGLYRP2*), which codes a peptidoglycan-hydrolytic
524 amidase that participates in antimicrobial immunity, hydrolysing the biologically
525 active peptidoglycan of the bacterial cell wall into inactive fragments [101, 102].
526 *PGLYRP2* is constitutively expressed in the liver in the presence of bacteria and
527 cytokines to be secreted into blood, acting as an immunity modulator [101, 102].
528 Thus, higher expression levels of *PGLYRP2* may suggest compromised
529 mechanisms against microbial infections by the immune system, whose

530 vulnerability could facilitate infection that ultimately activates *PGLYRP2*. In
531 concordance, a majority of the terms offered by functional enrichment and GO
532 term analysis put the spotlight on 3 downregulated genes (SLA class II
533 histocompatibility antigen, DQ haplotype D alpha chain; HLA class II
534 histocompatibility antigen, DQ beta 1 chain; and major histocompatibility
535 complex, class II, DR alpha), whose function participates in the activation of the
536 immune response via antigen binding and presenting to the T lymphocytes [103].
537 Therefore, underexpression of these genes can underpin a deficient capacity for
538 antigen presentation that could suppose immunological weakness. This situation
539 suggests a compromised immunological function in the vitrified progeny, which
540 ultimately may enhance the *PGLYRP2* as a consequence of higher susceptibility
541 to microbial infections due to diminished immunological sensibility. Curiously,
542 *PGLYRP2* have a conserved Zn^{2+}-binding site in the enzyme's catalytic groove,
543 which is crucial for the amidase activity. Thereby, the disturbed Zn metabolism
544 after embryo vitrification could also have an impact on the functionality of this
545 innate immunity modulator, so higher expression of *PGLYRP2* may also be an
546 attempt to compensate for deficient activity.
547
548 Focusing on the proteomic analysis, it also revealed some disturbed metabolic
549 pathways related with the lipid, but also glycan, metabolism. Among the biological
550 processes related to DEPs, we can signal the "ATP synthesis coupled proton
551 transport", whereas we can highlight the "ATPase activity" and the "mitochondrial
552 proton-transporting ATP synthase complex, coupling factor F0" terms, attending
553 to the molecular function and cellular component, respectively. KEEG pathway
554 analysis reveals that these terms are related to some downrepresented proteins

555 (*G1SEH7, G1U826, G1TX53, G1T9N2, O79431, G1TAP1*) involved in oxidative
556 phosphorylation (OXPHO). This metabolic process is carried out in the
557 mitochondria by ATP synthase complex, which is composed of 2 rotary motors,
558 the F0 and F1 subunits, whose joint performance is required for the correct
559 function of the complex [104, 105]. So, disturbed ATP synthase activity suggests
560 a mitochondrial dysfunction that could impair the *OXPHO* and ATP production. In
561 agreement, Feuer *et al.* [16] observed that mitochondrial dysfunction and *OXPHO*
562 changes were exhibited in the livers after IVF conception, reporting changes in
563 the ATP levels. It is important to indicate that *OXPHO* plays a key role in
564 processes such as energy production, generation of free radicals and apoptosis
565 [106], whose disturbances are found alone or in combination in most human
566 diseases such as intrauterine growth retardation, prematurity, low birth weight,
567 poor weight gain, major growth retardation, short stature and dwarfism [107-110].
568 Intriguingly, improvements in this mitochondrial function attenuated the postnatal
569 energy deficiency and resulted in normalisation of body weight gain [100].
570 Assuming this, DEPs involved in *OXPHO* suggested a disturbed energy
571 metabolism that might explain the lower growth curve presented by rabbits
572 obtained after transfer of vitrified embryos. Thus, assuming that vitrification
573 causes mitochondrial damages in the embryo, the resulting compromised
574 functionality of these organelles could be inherited by later tissue cells [111-113].
575 Furthermore, proteomic results showed some downrepresented DEPs involved
576 in the drug-metabolising mechanisms via cytochrome P450 in liver cells,
577 reinforcing the compromised liver detoxification function insinuated by KEGG
578 pathways of the transcriptomic comparison [114]. Finally, taking into account both
579 omic studies in this work, it is interesting to highlight that 17 DETs and 32 DEPs

580 are related to extracellular exosome GO term. Exosomes are membranous
581 vesicles secreted by liver cells that contain proteins, lipids and nucleic acids
582 coated with a lipid bilayer. Thus, the exosome load represents a snapshot of the
583 parental cell metabolism at the time of release and has been proposed as a
584 potential biomarker of liver disease [115]. So, this information reinforces the
585 finding that the metabolism and physiology of hepatic tissue was modified after
586 transfer of vitrified embryos. Proteomic analysis of these vesicles can offer
587 interesting information to the field, increasing the studies that evaluate the ART
588 effects through proteomic comparisons both in domestic animals [33-36], and
589 humans [37, 116].
590
591 Hence, we noted that some global results seem to have a common denominator.
592 Disturbed lipid metabolism and impaired mitochondrial function (energy
593 metabolism) in the liver could be ascribed to early placental insufficiency that
594 leads to foetal growth restriction [100, 117]. In this line, as we previously reported,
595 evidence for placental abnormality in foetuses was observed after transfer of
596 vitrified embryos [34, 35], probably due to preferential confinement of damaged
597 cells to the trophectoderm [118]. In fact, it has been reported that gene expression
598 related to lipid metabolism, steroidogenesis, cell differentiation and placentation
599 changed in blastocyst embryos following cryopreservation [68]. In this sense,
600 compromised placenta limits the availability of the critical substrates to the foetus
601 and retards development of the embryo and/or its organs during gestation. This
602 impaired organogenesis, particularly of the liver, could lead to permanent
603 changes in glucose and lipid metabolism, accompanied by a disturbance in the
604 oxidation of these substrates via *OXPHO*, which can affect the health of the

offspring and could continue into later developmental stages until adulthood [18, 98-100, 117, 119]. Therefore, disruption in normal development may result in organogenic errors that could incur permanent changes observable in adult life. In concordance, liver but also heart weight was lower after embryo vitrification. Similar phenotype modifications were described in mice after *in vitro* culture without serum in the culture medium [7]. Accordingly, lower blood pressure was exhibited by IVF mice [13]. Notably, structural remodelling of the heart was exhibited by IVF children compared to spontaneously conceived offspring [120]. Transcriptomic analysis of the IVF progeny heart tissue revealed 1361 downregulated genes [38], suggesting that both heart structure and its physiology became modified after ART. Worryingly, these differences are generally only found after a careful post-mortem examination of apparently normal individuals, suggesting that a masked compromised welfare may be occurring [11].

Conclusions

In conclusion, our experimental approach provides a broad overview that male progeny derived from vitrified embryo transfer manipulation technique have long-term consequences on growth rate and vital organ weights in adulthood, correlated with molecular signatures at transcriptomic and proteomic level. Today, a well-accepted hypothesis is that exposure of an organism to its environment at critical stages during development can trigger adaptive mechanisms, due to the active phenotypic plasticity of the embryo, resulting in a phenotypic variant of the individuals. This study should represent a significant step towards promoting a paradigm shift in characterisation of long-term

629 consequences of ART in adulthood, and thus opens the way to elucidating the
630 adaptive mechanisms of embryos from a systems biology perspective.
631

632 Acknowledgements

633 English text version revised by N. Macowan English Language Service.

References

1. Feuer SK, Rinaudo PF 2017 Physiological, metabolic and transcriptional postnatal phenotypes of in vitro fertilization (IVF) in the mouse. J Dev Orig Health Dis. 2017;8: 403-410.

2. Abdel-Latif ME, Bajuk B, Ward M, Oei JL, Badawi N, NSW & ACT Neonatal Intensive Care Units Audit Group. Neurodevelopmental outcomes of extremely premature infants conceived after assisted conception: a population based cohort study. Arch Dis Child Fetal Neonatal Ed. 2013;98: 205-11.

3. Fleming TP, Velazquez MA, Eckert JJ. Embryos, DOHaD and David Barker. J Dev Orig Health Dis. 2015;6: 377-83.

4. Chen M, Heilbronn LK 2017 The health outcomes of human offspring conceived by assisted reproductive technologies (ART). J Dev Orig Health Dis. 2017;8: 388-402.

5. Vrooman LA, Bartolomei MS. Can assisted reproductive technologies cause adult-onset disease? Evidence from human and mouse. Reprod Toxicol. 2017;68: 72-84.

6. Ecker DJ, Stein P, Xu Z, Williams CJ, Kopf GS, Bilker WB, et al. Long-term effects of culture of preimplantation mouse embryos on behavior. Proc Natl Acad Sci USA. 2004;101: 1595-1600.

653 7. Fernandez-Gonzalez R, Moreira P, Bilbao A, Jiménez A, Pérez-Crespo M,
654 Ramírez MA, et al. Long-term effect of in vitro culture of mouse embryos with
655 serum on mRNA expression of imprinting genes, development, and behavior.
656 Proc Natl Acad Sci U S A. 2004;101: 5880-5885.

657 8. Watkins AJ, Platt D, Papenbrock T, Wilkins A, Eckert JJ, Kwong WY, et al.
658 Mouse embryo culture induces changes in postnatal phenotype including raised
659 systolic blood pressure. Proc Natl Acad Sci U S A. 2007;104 5449-5454.

660 9. Scott KA, Yamazaki Y, Yamamoto M, Lin Y, Melhorn SJ, Krause EG, et al.
661 Glucose parameters are altered in mouse offspring produced by assisted
662 reproductive technologies and somatic cell nuclear transfer. Biol Reprod.
663 2010;83: 220-227.

664 10. 11 A, Miranda A, Fernandez-Gonzalez R, Pericuesta E, Laguna,
665 Gutierrez-Adan A. Male mice produced by in vitro culture have reduced fertility
666 and transmit organomegaly and glucose intolerance to their male offspring. Biol
667 Reprod. 2012;87: 1-9.

668 11. Calle A, Fernandez-Gonzalez R, Ramos-Ibeas P, Laguna-Barraza R,
669 Perez-Cerezales S, Bermejo-Alvarez P, et al. Long-term and transgenerational
670 effects of in vitro culture on mouse embryos. Theriogenology. 2012;77: 785-93.

671 12. Rexhaj E, Paoloni-Giacobino A, Rimoldi SF, Fuster DG, Anderegg M,
672 Somm E, et al. Mice generated by in vitro fertilization exhibit vascular dysfunction
673 and shortened life span. J Clin Invest. 2013;123: 5052-5060.

674 13. Donjacour A, Liu X, Lin W, Simbulan R, Rinaudo PF. In vitro fertilization
675 affects growth and glucose metabolism in a sex-specific manner in an outbred
676 mouse model. Biol Reprod. 2014;90: 80.

677 14. Chen M, Wu L, Wu F, Wittert GA, Norman RJ, Robker RL et al. Impaired
678 glucose metabolism in response to high fat diet in female mice conceived by in
679 vitro fertilization (IVF) or ovarian stimulation alone. PLoS One. 2014;9: e113155.

680 15. Feuer SK, Donjacour A, Simbulan RK, Lin W, Liu X, Maltepe E, et al.
681 Sexually dimorphic effect of in vitro fertilization (IVF) on adult mouse fat and liver
682 metabolomes. Endocrinology. 2014;155: 4554-4567.

683 16. Feuer SK, Liu X, Donjacour A, Lin W, Simbulan RK, Giritharan G, et al.
684 Use of a mouse in vitro fertilization model to understand the developmental
685 origins of health and disease hypothesis. Endocrinology. 2014;155: 1956-1969.

686 17. Li B, Chen S, Tang N, Xiao X, Huang J, Jiang F, et al. Assisted
687 Reproduction Causes Reduced Fetal Growth Associated with Downregulation of
688 Paternally Expressed Imprinted Genes That Enhance Fetal Growth in Mice. Biol
689 Reprod. 2016;94: 45.

690 18. Li B, Xiao X, Chen S, Huang J, Ma Y, Tang N, et al. Changes of
691 Phospholipids in Fetal Liver of Mice Conceived by In Vitro Fertilization. Biol
692 Reprod. 2016;94: 105.

693 19. Giorgione V, Parazzini F, Fesslova V, Cipriani S, Candiani M, Inversetti A,
694 et al. Congenital heart defects in IVF/ICSI pregnancy: a systematic review and
695 meta-analysis. Ultrasound Obstet Gynecol. 2017;51: 33-42.

696 20. Servick K. Unsettled questions trail IVF's success. Science. 2014;345:
697 744-6.

698 21. Wong KM, Mastenbroek S, Repping S. Cryopreservation of human
699 embryos and its contribution to in vitro fertilization success rates. Fertil Steril.
700 2014;102: 19-26.

701 22. Sparks AE. Human embryo cryopreservation-methods, timing, and other
702 considerations for optimizing an embryo cryopreservation program. Semin
703 Reprod Med. 2015;33: 128-44.

704 23. Dulioust E, Toyama K, Busnel MC, Moutier R, Carlier M, Marchaland C, et
705 al. Long-term effects of embryo freezing in mice. Proc Natl Acad Sci USA.
706 1995;92: 589-93.

707 24. Hipp H, Crawford S, Kawwass JF, Chang J, Kissin DM, Jamieson DJ. First
708 trimester pregnancy loss after fresh and frozen in vitro fertilization cycles. Fertil
709 Steril. 2016;105: 722-728.

710 25. Wong KM, van Wely M, Mol F, Repping S, Mastenbroek S. Fresh versus
711 frozen embryo transfers in assisted reproduction. Cochrane Database Syst Rev.
712 2017;3: CD011184.

713 26. Maheshwari A, Pandey S, Amalraj Raja E, Shetty A, Hamilton,
714 Bhattacharya S. Is frozen embryo transfer better for mothers and babies? Can
715 cumulative meta-analysis provide a definitive answer? Hum Reprod Update.
716 2018;24: 35-58.

717 27. Arnold GJ, Frohlich T. Dynamic proteome signatures in gametes, embryos
718 and their maternal environment. Reprod Fertil Dev. 2011;23: 81-93.

719 28. Gad A, Besenfelder U, Rings F, Ghanem N, Salilew-Wondim D, Hossain
720 MM, et al. Effect of reproductive tract environment following controlled ovarian
721 hyperstimulation treatment on embryo development and global transcriptome
722 profile of blastocysts: implications for animal breeding and human assisted
723 reproduction. Hum Reprod. 2011;26: 1693-707.

724 29. Driver AM, Peñagaricano F, Huang W, Ahmad KR, Hackbart KS, Wiltbank
725 MC, et al. RNA-Seq analysis uncovers transcriptomic variations between
726 morphologically similar in vivo- and in vitro-derived bovine blastocysts. BMC
727 Genomics. 2012;13: 118.

728 30. Feuer S, Liu X, Donjacour A, Simbulan R, Maltepe E, Rinaudo. Common
729 and specific transcriptional signatures in mouse embryos and adult tissues
730 induced by in vitro procedures. Reproduction. 2017;153: 107-122.

731 31. Feuer SK, LiuX, Donjacour A, Simbulan R, Maltepe E, Rinaudo.
732 Transcriptional signatures throughout development: The effects of mouse
733 embryo manipulation in vitro. Reproduction. 2017;153: 107-122.

734 32. Duranthon V, Chavatte-Palmer P. Long term effects of ART: What do
735 animals tell us? Mol Reprod Dev. 2018;85: 348-368.

736 33. Sui L, An L, Tan K, Wang Z, Wang S, Miao K, et al. Dynamic proteomic
737 profiles of in vivo- and in vitro-produced mouse postimplantation extraembryonic
738 tissues and placentas. Biol Reprod. 2014;91: 155.

739 34. Saenz-de-Juano MD, Marco-Jimenez F, Schmaltz-Panneau B, Jimenez-
740 Trigos E, Viudes-de-Castro MP, Peñaranda DS, et al. Vitrification alters rabbit
741 foetal placenta at transcriptomic and proteomic level. Reproduction. 2014;147:
742 789-801.

743 35. Saenz-de-Juano MD, Vicente JS, Hollung, Marco-Jiménez F. Effect of
744 Embryo Vitrification on Rabbit Foetal Placenta Proteome during Pregnancy.
745 PLoS One. 2015;10: e0125157.

746 36. Nie J, An L, Miao K, Hou Z, Yu Y, Tan K, et al. Comparative analysis of
747 dynamic proteomic profiles between in vivo and in vitro produced mouse embryos
748 during postimplantation period. J Proteome Res. 2013;12: 3843-56.

749 37. Gao Q, Pan HT, Lin XH, Zhang JY, Jiang Y, Tian S, et al. Altered protein
750 expression profiles in umbilical veins: insights into vascular dysfunctions of the
751 children born after in vitro fertilization. Biol Reprod. 2014;91: 71.

752 38. Feuer S, Rinaudo P. From Embryos to Adults: A DOHaD Perspective on
753 In Vitro Fertilization and Other Assisted Reproductive Technologies. Healthcare
754 (Basel). 2016;4: 51.

755 39. Strata F, Giritharan G, Sebastiano FD, Piane LD, Kao CN, Donjacour A,
756 et al. Behavior and brain gene expression changes in mice exposed to
757 preimplantation and prenatal stress. Reprod Sci. 2015;22: 23-30.

758 40. Gkourogianni A, Kosteria I, Telonis AG, Margeli A, Mantzou E, Konsta M,
759 et al. Plasma metabolomic profiling suggests early indications for predisposition
760 to latent insulin resistance in children conceived by ICSI. PLoS One. 2014;9:
761 e94001.

762 41. Vicente JS, Viudes-de-Castro MP, García ML. In vivo survival rate of rabbit
763 morulae after vitrification in a medium without serum protein. Reproduction,
764 Nutrition, Development. 1999;39: 657–662.

765 42. Besenfelder U, Brem G. Laparoscopic embryo transfer in rabbits. Journal
766 of Reproduction and Fertility. 1993;99: 53–56.

767 43. Blasco A, Gomez E. A note on growth curves of rabbit lines selected on
768 growth rate or litter size. Anim Prod. 1993;57: 332–4.

769 44. Kilborn SH, Trudel G, Uhthoff H. Review of growth plate closure compared
770 with age at sexual maturity and lifespan in laboratory animals. Contemp Top Lab
771 Anim Sci. 2002;41: 21-6.

772 45. Laird AK. Postnatal growth of birds and mammals. Growth 1965;30: 349-
773 63.

774 46. Andrews S. FastQC: a quality control tool for high throughput sequence
775 data. Available online at:
776 http://www.bioinformatics.babraham.ac.uk/projects/fastqc. 2010.

777 47. Kim D, Langmead B, Salzberg SL. HISAT: a fast spliced aligner with low
778 memory requirements. Nature Methods. 2015;12: 357-360.

779 48. Pertea M, Pertea GM, Antonescu CM, Chang TC, Mendell JT, Salzberg
780 SL. StringTie enables improved reconstruction of a transcriptome from RNA-seq
781 reads. Nature Biotechnology. 2015;33: 290-5.

782 49. Robinson MD, McCarthy DJ, Smyth GK. edgeR: a Bioconductor package
783 for differential expression analysis of digital gene expression data. Bioinformatics.
784 2010;26: 139-140.

785 50. Wang YE, Kutnetsov L, Partensky A, Farid J, Quackenbush J. WebMeV:
786 A Cloud Platform for Analyzing and Visualizing Cancer Genomic Data. Cancer
787 Res. 2017;77: e11-e14.

788 51. Metsalu T, Vilo J. ClustVis: a web tool for visualizing clustering of
789 multivariate data using Principal Component Analysis and heatmap. Nucleic
790 Acids Res. 2015;43: W566-70.

52. Hyun H, Park J, Willis K, Park JE, Lyle LT, Lee W, et al. Surface modification of polymer nanoparticles with native albumin for enhancing drug delivery to solid tumors. Biomaterials. 2018;180: 206-224.

53. Canovas S, Ivanova E, Romar R, García-Martínez S, Soriano-Úbeda C, García-Vázquez FA, et al. DNA methylation and gene expression changes derived from assisted reproductive technologies can be decreased by reproductive fluids. Elife. 2017;6: e23670.

54. Kleijkers SH, van Montfoort AP, Smits LJ, Viechtbauer W, Roseboom TJ, Nelissen EC, et al. IVF culture medium affects post-natal weight in humans during the first 2 years of life. Hum Reprod. 2014;29: 661-9.

55. Lazaraviciute G, Kauser M, Bhattacharya S, Haggarty P, Bhattacharya S. A systematic review and meta-analysis of DNA methylation levels and imprinting disorders in children conceived by IVF/ICSI compared with children conceived spontaneously. Hum Reprod Update. 2014;20: 840-52.

56. Song S, Ghosh J, Mainigi M, Turan N, Weinerman R, Truongcao M, et al. DNA methylation differences between in vitro- and in vivo-conceived children are associated with ART procedures rather than infertility. Clinical Epigenetics. 2015;7: 41.

57. Lavara R, Baselga M, Marco-Jiménez F, Vicente JS. Embryo vitrification in rabbits: Consequences for progeny growth. Theriogenology. 2015;84: 674-80.

811 58. Forsman A. Rethinking phenotypic plasticity and its consequences for
812 individuals, populations and species. Heredity (Edinb). 2015;115: 276-84.

813 59. Rienzi L, Gracia C, Maggiulli R, LaBarbera AR, Kaser DJ, Ubaldi FM, et
814 al. Oocyte, embryo and blastocyst cryopreservation in ART: systematic review
815 and meta-analysis comparing slow-freezing versus vitrification to produce
816 evidence for the development of global guidance. Hum Reprod Update. 2017;23:
817 139-155.

818 60. Alikani M. Cryostorage of human gametes and embryos: a reckoning.
819 Reprod Biomed Online. 2018;37: 1-3.

820 61. Shapiro BS, Daneshmand ST, Garner FC, Aguirre M, Hudson C. Clinical
821 rationale for cryopreservation of entire embryo cohorts in lieu of fresh transfer.
822 Fertil Steril. 2014;102: 3-9.

823 62. Roque M, Valle M, Kostolias A, Sampaio M, Geber S. Freeze-all cycle in
824 reproductive medicine: current perspectives. JBRA Assist Reprod. 2017;21: 49-
825 53.

826 63. Maheshwari A, Raja EA, Bhattacharya S. Obstetric and perinatal
827 outcomes after either fresh or thawed frozen embryo transfer: an analysis of
828 112,432 singleton pregnancies recorded in the Human Fertilisation and
829 Embryology Authority anonymized dataset. Fertil Steril. 2016;106: 1703-1708.

830 64. Vidal M, Vellvé K, González-Comadran M, Robles A, Prat M, Torné M, et
831 al. Perinatal outcomes in children born after fresh or frozen embryo transfer: a
832 Catalan cohort study based on 14,262 newborns. Fertil Steril. 2017;107: 940-
833 947.

834 65. Auroux M. Long-term effects in progeny of paternal environment and of
835 gamete/embryo cryopreservation. Hum Reprod Update. 2000;6: 550-63.

836 66. Auroux M, Cerutti I, Ducot B, Loeuillet A. Is embryo-cryopreservation really
837 neutral? A new long- term effect of embryo freezing in mice: protection of adults
838 from induced cancer according to strain and sex. Reprod Toxicol. 2004;18: 813-
839 818.

840 67. Vicente JS, Saenz-de-Juano MD, Jiménez-Trigos E, Viudes-de-Castro
841 MP, Peñaranda DS, et al. Rabbit morula vitrification reduces early foetal growth
842 and increases losses throughout gestation. Cryobiology. 2013;67: 321-6.

843 68. Gupta A, Singh J, Dufort I, Robert C, Dias FCF, Anzar M. Transcriptomic
844 difference in bovine blastocysts following vitrification and slow freezing at morula
845 stage. PLoS One. 2017;12: e0187268.

846 69. Li HZ, Qiao J, Chi HB, Chen XN, Liu P, Ma CH. Comparison of the major
847 malformation rate of children conceived from cryopreserved embryos and fresh
848 embryos. Chin Med J (Engl). 2010;123: 1893-7.

849 70. Huang B, Qian K, Li Z, Yue J, Yang W, Zhu G, et al. Neonatal outcomes
850 after early rescue intracytoplasmic sperm injection: an analysis of a 5-year period.
851 Fertil Steril. 2015;103: 1432-7.

852 71. Yang X, Li Y, Li C, Zhang W. Current overview of pregnancy complications
853 and live-birth outcome of assisted reproductive technology in mainland China.
854 Fertil Steril. 2014;101: 385-91.

855 72. Yang M, Fan XB, Wu JN, Wang JM. Association of assisted reproductive
856 technology and multiple pregnancies with the risks of birth defects and stillbirth:
857 A retrospective cohort study. Sci Rep. 2018;8: 8296.

858 73. Wennerholm UB, Söderström-Anttila V, Bergh C, Aittomäki K, Hazekamp
859 J, Nygren KG, et al. Children born after cryopreservation of embryos or oocytes:
860 a systematic review of outcome data. Hum Reprod. 2009;24: 2158-72.

861 74. Pelkonen S, Gissler M, Koivurova S, Lehtinen S, Martikainen H,
862 Hartikainen AL, et al. Physical health of singleton children born after frozen
863 embryo transfer using slow freezing: a 3-year follow-up study. Hum Reprod.
864 2015;30: 2411-8.

865 75. Belva F, Bonduelle M, Roelants M, Verheyen G, Van Landuyt L. Neonatal
866 health including congenital malformation risk of 1072 children born after vitrified
867 embryo transfer. Hum Reprod. 2016;31: 1610-20.

868 76. Gidenne T, Combes S, Feugier A, Jehl N, Arveux P, Boisot P, et al. Feed
869 restriction strategy in the growing rabbit. 2. Impact on digestive health, growth
870 and carcass characteristics. Animal. 2009;3: 509-15.

871 77. Chen Z, Robbins KM, Wells KD, Rivera RM. Large offspring syndrome: a
872 bovine model for the human loss-of-imprinting overgrowth syndrome Beckwith-
873 Wiedemann. Epigenetics. 2013;8: 591-601.

874 78. Pinborg A, Loft A, Aaris Henningsen AK, Rasmussen S, Andersen. Infant
875 outcome of 957 singletons born after frozen embryo replacement: the Danish
876 National Cohort Study 1995-2006. Fertil Steril. 2010;94: 1320-7.

877 79. Spijkers S, Lens JW, Schats R, Lambalk CB. Fresh and Frozen-Thawed
878 Embryo Transfer Compared to Natural Conception: Differences in Perinatal
879 Outcome. Gynecol Obstet Invest. 2017;82: 538-546.

880 80. Cifre J, Baselga M, Gómez EA, García ML. Effect of embryo
881 cryopreservation techniques on reproductive and growth traits in rabbits. Ann
882 Zootech. 1999;48: 15-24.

883 81. Mahsoudi B, Li A, O'Neill C. Assessment of the long-term and
884 transgenerational consequences of perturbing preimplantation embryo
885 development in mice. Biol Reprod. 2007;77: 889-96.

886 82. Bracewell-Milnes T, Saso S, Abdalla H, Nikolau D, Norman-Taylor J,
887 Johnson M, et al. Metabolomics as a tool to identify biomarkers to predict and
888 improve outcomes in reproductive medicine: a systematic review. Hum Reprod
889 Update. 2017;23: 723-736.

890 83. Frank SJ. Growth hormone, insulin-like growth factor I, and growth: local
891 knowledge. Endocrinology. 2007;148: 1486-8.

892 84. Mak RH, Cheung WW, Roberts CT Jr. The growth hormone-insulin-like
893 growth factor-I axis in chronic kidney disease. Growth Horm IGF Res. 2008;18:
894 17-25.

895 85. Baik M, Yu JH, Hennighausen L.Growth hormone-STAT5 regulation of
896 growth, hepatocellular carcinoma, and liver metabolism. Ann N Y Acad Sci.
897 2011;1229: 29-37.

898 86. Davis SR, Cousins RJ. Metallothionein expression in animals: A
899 physiological perspective on function. J. Nutr. 2000;130: 1085-1088.

900 87. Kadota Y, Aki Y, Toriuchi Y, Mizuno Y, Kawakami T, Sato M, et al.
901 Deficiency of metallothionein-1 and -2 genes shortens the lifespan of the 129/Sv
902 mouse strain. Exp Gerontol. 2015;66: 21-4.

903 88. She Y, Huang Q, Li D, Piao X. Effects of proteinate complex zinc on growth
904 performance, hepatic and splenic trace elements concentrations, antioxidative
905 function and immune functions in weaned piglets. Asian-Australas J Anim Sci.
906 2017;30: 1160-1167.

907 89. Hill GM, Mahan DC, Jolliff JS. Comparison of organic and inorganic zinc
908 sources to maximize growth and meet the zinc needs of the nursery pig. J Anim
909 Sci. 2014;92: 1582-94.

910 90. Shaikhkhalil AK, Curtiss J, Puthoff TD,Valentine CJ. Enteral zinc
911 supplementation and growth in extremely-low-birth-weight infants with chronic
912 lung disease. J Pediatr Gastroenterol Nutr. 2014;58: 183-7.

913 91. Zhao CY, Tan SX, Xiao XY, Qiu XS, Pan JQ, Tang ZX. Effects of dietary
914 zinc oxide nanoparticles on growth performance and antioxidative status in
915 broilers. Biol Trace Elem Res. 2014;160: 361-7.

916 92. Martínez MM, Hill GM, Link JE, Raney NE, Tempelman RJ, Ernst CW.
917 Pharmacological zinc and phytase supplementation enhance metallothionein
918 mRNA abundance and protein concentration in newly weaned pigs. J Nutr.
919 2004;134: 538-44.

920 93. El-Farghali O, El-Wahed MA, Hassan NE, Imam S, Alian K. Early Zinc
921 Supplementation and Enhanced Growth of the Low-Birth Weight Neonate. Open
922 Access Maced J Med Sci. 2015;3: 63-8.

923 94. Meesapyodsuk D, Qiu X. The front-end desaturase: structure, function,
924 evolution and biotechnological use. Lipids. 2012;47: 227-37.

925 95. Chimhashu T, Malan L, Baumgartner J, van Jaarsveld PJ, Galetti V,
926 Moretti D, et al. Sensitivity of fatty acid desaturation and elongation to plasma
927 zinc concentration: a randomised controlled trial in Beninese children. Br J Nutr.
928 2018;119: 610-619.

929 96. Park HG, Engel MG, Vogt-Lowell K, Lawrence P, Kothapalli KS, Brenna
930 JT. The role of fatty acid desaturase (FADS) genes in oleic acid metabolism:
931 FADS1 Δ7 desaturates 11-20:1 to 7,11-20:2. Prostaglandins Leukot Essent Fatty
932 Acids. 2018;128: 21-25.

933 97. Bistrian BR. Clinical aspects of essential fatty acid metabolism: Jonathan
934 Rhoads Lecture. JPEN J Parenter Enteral Nutr. 2003;27: 168-75.

935 98. Barker D J, Martyn CN, Osmond C, Hales CN, Fall CH. Growth in utero
936 and serum cholesterol concentrations in adult life. BMJ. 1993;307: 1524-1527.

937 99. Serrano A, Decara JM, Fernandez-Gonzalez R, López-Cardona AP,
938 Pavón FJ, Orio L, et al. Hyperplastic obesity and liver steatosis as long-term
939 consequences of suboptimal in vitro culture of mouse embryos. Biol Reprod.
940 2014;91: 30.

941 100. Zhang H, Li Y, Su W, Ying Z, Zhou L, Zhang L, et al. Resveratrol
942 attenuates mitochondrial dysfunction in the liver of intrauterine growth retarded
943 suckling piglets by improving mitochondrial biogenesis and redox status. Mol Nutr
944 Food Res. 2017;61: In press. https://doi.org/10.1002/mnfr.201600653.

945 101. Dziarski R, Gupta D. Review: Mammalian peptidoglycan recognition
946 proteins (PGRPs) in innate immunity. Innate Immun. 2010;16: 168-74.

947 102. Lee J, Geddes K, Streutker C, Philpott DJ, Girardin SE. Role of mouse
948 peptidoglycan recognition protein PGLYRP2 in the innate immune response to
949 Salmonella enterica serovar Typhimurium infection in vivo. Infect Immun.
950 2012;80: 2645-54.

951 103. Trombetta ES, Mellman I. Cell biology of antigen processing in vitro and in
952 vivo. Annu Rev Immunol. 2005;23: 975-1028.

953 104. Watt IN, Montgomery MG, Runswick MJ, Leslie AG, Walker JE.
954 Bioenergetic cost of making an adenosine triphosphate molecule in animal
955 mitochondria. Proc Natl Acad Sci U S A. 2010;107: 16823-7.

956 105. Martin J, Hudson J, Hornung T, Frasch WD. Fo-driven Rotation in the ATP
957 Synthase Direction against the Force of F1 ATPase in the FoF1 ATP Synthase.
958 J Biol Chem. 2015;290: 10717-28.

959 106. Hüttemann M, Lee I, Samavati L, Yu H, Doan JW. Regulation of
960 mitochondrial oxidative phosphorylation through cell signaling. Biochim Biophys
961 Acta. 2007;1773: 1701-20.

962 107. Munnich A, Rustin P. Clinical spectrum and diagnosis of mitochondrial
963 disorders. Am J Med Genet. 2001;106: 4 -17.

964 108. von Kleist-Retzow JC, Cormier-Daire V, Viot G, Goldenberg A, Mardach
965 B, Amiel J, et al. Antenatal manifestations of mitochondrial respiratory chain
966 deficiency. J Pediatr. 2003;143: 208 -212.

967 109. Gibson K, Halliday JL, Kirby DM, Yaplito-Lee J, Thorburn DR, Boneh A.
968 Mitochondrial oxidative phosphorylation disorders presenting in neonates: clinical
969 manifestations and enzymatic and molecular diagnoses. Pediatrics. 2008;122:
970 1003-8.

971 110. Abu-Libdeh B, Douiev L, Amro S, Shahrour M, Ta-Shma A, Miller C, et al.
972 Mutation in the COX4I1 gene is associated with short stature, poor weight gain
973 and increased chromosomal breaks, simulating Fanconi anemia. Eur J Hum
974 Genet. 2017;25: 1142-1146.

975 111. Lei T, Guo N, Tan MH, Li YF. Effect of mouse oocyte vitrification on
976 mitochondrial membrane potential and distribution. J Huazhong Univ Sci
977 Technolog Med Sci. 2014;34: 99-102.

978 112. Chiaratti MR, Garcia BM, Carvalho KF, Machado TS, Ribeiro FKDS,
979 Macabelli CH. The role of mitochondria in the female germline: Implications to
980 fertility and inheritance of mitochondrial diseases. Cell Biol Int. 2018;42: 711-724.

981 113. Succu S, Gadau SD, Serra E, Zinellu A, Carru C, Porcu C, et al. A recovery
982 time after warming restores mitochondrial function and improves developmental
983 competence of vitrified ovine oocytes. Theriogenology. 2018;110: 18-26.

984 114. Almazroo OA, Miah MK, Venkataramanan R. Drug Metabolism in the
985 Liver. Clin Liver Dis. 2017;21: 1-20.

986 115. Szabo G, Momen-Heravi F. Extracellular vesicles in liver disease and
987 potential as biomarkers and therapeutic targets. Nat Rev Gastroenterol Hepatol.
988 2017;14: 455-466.

989 116. Kosteria I, Tsangaris GT, Gkourogianni A, Anagnostopoulos A,
990 Papadopoulou A, Papassotiriou I, et al. Proteomics of Children Born After
991 Intracytoplasmic Sperm Injection Reveal Indices of an Adverse Cardiometabolic
992 Profile. J Endocr Soc. 2017;1: 288-301.

993 117. Peterside IE, Selak MA, Simmons RA. Impaired oxidative phosphorylation
994 in hepatic mitochondria in growth-retarded rats. Am J Physiol Endocrinol Metab.
995 2003;285: E1258-66.

996 118. Bazrgar M, Gourabi H, Valojerdi MR, Yazdi PE, Baharvand H. Self-
997 correction of chromosomal abnormalities in human preimplantation embryos and
998 embryonic stem cells. Stem Cells Dev. 2013;22: 2449-56.

999 119. Shekhawat PS, Matern D, Strauss AW. Fetal fatty acid oxidation disorders,
1000 their effect on maternal health and neonatal outcome: impact of expanded
1001 newborn screening on their diagnosis and management. Pediatr Res. 2005;57:
1002 78R-86R.

1003 120. Zhou J, Liu H, Gu HT, Cui YG, Zhao NN, Chen J, et al. Association of
1004 cardiac development with assisted reproductive technology in childhood: a
1005 prospective single-blind pilot study. Cell Physiol Biochem. 2014;34: 988-1000.

1006

Figure Legends

Fig 1. Experimental design. Two experimental groups were developed; (i) animals born from vitrified embryos transferred to the surrogate mothers and (ii) animals born after natural conception. In both groups and after delivery, male offspring were weighed every week until the adulthood (growth performance). At adulthood, haematological and organs weight comparison was performed. In addition, transcriptomic and proteomic comparative analysis of liver tissue was developed.

Fig 2. Growth curves from vitrified-transferred embryos and naturally conceiving.

Fig 3. Differences in body weight between naturally conceived (NC) and vitrified-transferred (VT) groups during development, computed as NC-VT.

Fig 4. Molecular analysis in liver samples obtained from adult males derived from vitrified-transferred embryos and naturally conceiving. (A) Principal component analysis of the transcriptome. (B) Heat-Map clustering of the transcriptome. (C) Principal component analysis of the proteome. (D) Heat-Map clustering of the proteome. The representation of sample variability between the experimental groups was performed taking into account only the differentially expressed transcripts and proteins and the transcripts or proteins absent in specific groups.

1032

1033

1034

Tables

Table 1. Body weight and dissection data of adult males derived from vitrified-transferred embryos and naturally conceiving.

Traits	Vitrified-transferred (n=30)	Naturally conceived (n=35)
Body Weight (Kg)	5.3 ± 0.11[b]	5.7 ± 0.10[a]
Kidneys (g)	22.3 ± 0.42	22.7 ± 0.45
Liver (g)	92.8 ± 2.37[b]	102.1 ± 2.51[a]
Spleen (g)	1.3 ± 0.07	1.4 ± 0.08
Lungs (g)	26.7 ± 1.13	25.6 ± 1.20
Heart (g)	11.6 ± 0.44[b]	13.1 ± 0.43[a]
Gonads (g)	6.9 ± 0.34	6.2 ± 0.36
Adrenal Glands (g)	0.7 ± 0.03	0.6 ± 0.04

n represents the number of samples. All the organ weights were corrected by body weight. [a,b] Values in the same row with different superscript are significantly different ($p < 0.05$). Data are expressed as least-square mean ± standard error of means.

Table 2. Haematological comparison between vitrified-transferred and naturally conceived groups.

Parameters	Vitrified-transferred (n=10)	Naturally conceived (n=10)	p-value
WBC (10^3/mm^3)	12.2 ± 1.49	13.6 ± 1.49	0.491
LYM (10^3/mm^3)	6.8 ± 1.46	7.7 ± 1.46	0.663
MON (10^3/mm^3)	1.6 ± 0.143	1.8 ± 0.143	0.221
GRA (10^3/mm^3)	3.8 ± 0.38	4.15 ± 0.38	0.573
RBC (10^6/mm^3)	5.8 ± 0.095	5.9 ± 0.095	0.866
HTO (%)	40.6 ± 1.17	41.1 ± 1.17	0.812

WBC: White Blood Cells; LYM: Lymphocytes, MON: Monocytes, GRA: Granulocytes (10^3/mm^3), RBC: Red Blood Cells, HTO: Haematocrit. Data are expressed as least-square means ± standard error of means.

1058 **Table 3. Differentially expressed transcripts in the liver tissue.**

Gene accession	Gene name	Ratio*
ENSOCUG00000007555	Peptidoglycan recognition protein 2(PGLYRP2)	9.705
ENSOCUG00000012831	Insulin-like growth factor binding protein 1(IGFBP1)	2.972
ENSOCUG00000025112	Heat shock 70 kda protein 1B(LOC100354037)	2.799
ENSOCUG00000013296	Growth arrest and DNA damage inducible gamma(GADD45G)	2.734
ENSOCUG00000005465	Nocturnin(NOCT)	2.648
ENSOCUG00000008253	Tissue factor pathway inhibitor(TFPI)	2.434
ENSOCUG00000023743	Heat shock 70 kda protein 1B(LOC100354435)	2.244
ENSOCUG00000024474	L-gulonolactone oxidase(LOC100341843)	2.069
ENSOCUG00000007999	Dual specificity phosphatase 1(DUSP1)	2.03
ENSOCUG00000027233	Uncharacterised LOC100346308(LOC100346308)	1.985
ENSOCUG00000007130	Solute carrier family 25 member 25(SLC25A25)	1.959
ENSOCUG00000011201	CYP4B1-like isozyme short form(CYP4B1)	1.916
ENSOCUG00000009725	Acyl-coa wax alcohol acyltransferase 1(AWAT1)	1.905
ENSOCUG00000022168	Serine dehydratase(SDS)	1.864
ENSOCUG00000029130	Cytochrome P450 2C1(CYP2C1)	1.815
ENSOCUG00000004733	Prostaglandin-E(2) 9-reductase-like(PGER2)	1.73
ENSOCUG00000015313	Cytochrome c oxidase protein 20 homolog(LOC100349428)	1.673
ENSOCUG00000006009	Acyl-coenzyme A thioesterase 1(LOC100344509)	1.648
ENSOCUG00000014197	Macrophage scavenger receptor 1(MSR1)	1.642
ENSOCUG00000000125	Pleckstrin homology and FYVE domain containing 1(PLEKHF1)	1.508
ENSOCUG00000016772	DNA damage inducible transcript 4(DDIT4)	1.468
ENSOCUG00000008419	Solute carrier family 25 member 30(SLC25A30)	1.393
ENSOCUG00000006521	Chromosome unknown open reading frame, human c10orf10(LOC100349113)	1.372
ENSOCUG00000015352	Energy homeostasis associated(ENHO)	1.285
ENSOCUG00000003400	ZFP36 ring finger protein(ZFP36)	1.259
ENSOCUG00000027981	ISG15 ubiquitin-like modifier(ISG15)	1.248

ENSOCUG00000012690	Heat shock protein family B (small) member 1(HSPB1)	1.229
ENSOCUG00000023425	Alpha-fetoprotein(LOC103350776)	1.201
ENSOCUG00000001673	Triokinase and FMN cyclase(TKFC)	-1.214
ENSOCUG00000015864	Actin binding LIM protein 1(ABLIM1)	-1.214
ENSOCUG00000014326	Prostaglandin-E(2) 9-reductase-like(LOC100352716)	-1.234
ENSOCUG00000002480	SLA class II histocompatibility antigen, DQ haplotype D alpha chain(LOC100343144)	-1.246
ENSOCUG00000003477	Protein phosphatase 1 regulatory subunit 3B(PPP1R3B)	-1.256
ENSOCUG00000027184	Carbonyl reductase 1(CBR1)	-1.278
ENSOCUG00000015853	Glutaredoxin(GLRX)	-1.318
ENSOCUG00000004928	Transforming growth factor beta induced(TGFBI)	-1.34
ENSOCUG00000017688	Phosphoprotein enriched in astrocytes 15(PEA15)	-1.34
ENSOCUG00000015944	Complement factor properdin(CFP)	-1.342
ENSOCUG00000013069	ELOVL fatty acid elongase 6(ELOVL6)	-1.36
ENSOCUG00000009103	Major histocompatibility complex, class II, DR alpha(RLA-DR-ALPHA)	-1.362
ENSOCUG00000015051	Protein phosphatase 1 regulatory subunit 3C(PPP1R3C)	-1.381
ENSOCUG00000010633	Heme oxygenase 1(HMOX1)	-1.385
ENSOCUG00000021411	Tsukushi, small leucine rich proteoglycan(TSKU)	-1.401
ENSOCUG00000002485	HLA class II histocompatibility antigen, DQ beta 1 chain(LOC100351163)	-1.404
ENSOCUG00000000637	Myosin light chain 9(MYL9)	-1.415
ENSOCUG00000003858	Glycine N-methyltransferase(GNMT)	-1.432
ENSOCUG00000008193	Actin, alpha 2, smooth muscle, aorta(ACTA2)	-1.433
ENSOCUG00000027916	Frizzled class receptor 5(FZD5)	-1.436
ENSOCUG00000026406	Butyrophilin subfamily 1 member A1-like(LOC108175832)	-1.481
ENSOCUG00000013643	PDZ and LIM domain 1(PDLIM1)	-1.482
ENSOCUG00000006416	Nuclear receptor subfamily 0 group B member 2(NR0B2)	-1.518
ENSOCUG00000004137	Protease, serine 23(PRSS23)	-1.546
ENSOCUG00000016746	Interleukin 1 receptor type 2(IL1R2)	-1.548

ENSOCUG00000015138	Complement component 1, q subcomponent, C chain(C1QC)	-1.563
ENSOCUG00000008491	Testin LIM domain protein(TES)	-1.57
ENSOCUG00000010299	Cysteine and glycine rich protein 1(CSRP1)	-1.643
ENSOCUG00000025273	Liver carboxylesterase 2(LOC100343300)	-1.658
ENSOCUG00000025132	60S ribosomal protein l23a(LOC108177184)	-1.668
ENSOCUG00000006893	Macrophage receptor with collagenous structure(MARCO)	-1.673
ENSOCUG00000008498	Uridine phosphorylase 2(UPP2)	-1.706
ENSOCUG00000016964	Matrix Gla protein(MGP)	-1.728
ENSOCUG00000008841	Glutamate-ammonia ligase(GLUL)	-1.744
ENSOCUG00000012866	TEF, PAR bzip transcription factor(TEF)	-1.838
ENSOCUG00000003212	Tumour suppressor candidate 3(TUSC3)	-1.87
ENSOCUG00000025241	Liver carboxylesterase 2-like(LOC100357214)	-1.872
ENSOCUG00000016651	AXL receptor tyrosine kinase(AXL)	-1.888
ENSOCUG00000000763	Phospholipase A2 group VII(PLA2G7)	-1.896
ENSOCUG00000010936	Chromosome unknown open reading frame, human c16orf89(LOC100353142)	-1.943
ENSOCUG00000000161	SH3 domain binding protein 2(SH3BP2)	-1.964
ENSOCUG00000000313	Ovostatin homolog 2(LOC100348825)	-2.0
ENSOCUG00000026714	CD5 molecule like(CD5L)	-2.044
ENSOCUG00000014801	Acyl-coa desaturase(LOC100346561)	-2.083
ENSOCUG00000003903	Centromere protein U(CENPU)	-2.128
ENSOCUG00000000092	Serpin family F member 1(SERPINF1)	-2.174
ENSOCUG00000011970	Transgelin(TAGLN)	-2.297
ENSOCUG00000005174	Dermatopontin(DPT)	-2.299
ENSOCUG00000014432	Ectonucleotide pyrophosphatase/phosphodiesterase 3(ENPP3)	-2.37
ENSOCUG00000002707	MID1 interacting protein 1(MID1IP1)	-2.415
ENSOCUG00000015162	Microfibrillar associated protein 4(MFAP4)	-2.424
ENSOCUG00000015057	Macrophage expressed 1(MPEG1)	-2.518
ENSOCUG00000012264	Collagen type I alpha 2 chain(COL1A2)	-2.565
ENSOCUG00000015836	Myelin protein zero like 2(MPZL2)	-2.648

ENSOCUG00000004172	V-set and immunoglobulin domain containing 4(VSIG4)	-2.705
ENSOCUG00000017620	Serum amyloid protein A(LOC100009259)	-2.708
ENSOCUG00000001375	Acyl-coa desaturase(LOC100346046)	-2.766
ENSOCUG00000010198	Tropomyosin 2 (beta)(TPM2)	-2.798
ENSOCUG00000002924	Galectin 3(LGALS3)	-2.924
ENSOCUG00000012902	Glutathione S-transferase Yc(LOC100353428)	-2.984
ENSOCUG00000007516	6-phosphofructo-2-kinase/fructose-2,6-biphosphatase 3(PFKFB3)	-3.205
ENSOCUG00000012881	Collagen type I alpha 1 chain(COL1A1)	-3.737
ENSOCUG00000005830	HIG1 hypoxia inducible domain family member 1A(HIGD1A)	-3.933
ENSOCUG00000013412	C-C motif chemokine 7(LOC103351517)	-4.361
ENSOCUG00000029235	Metallothionein-1A(LOC100343802)	-5.017
ENSOCUG00000021209	Metallothionein-2D(LOC100343557)	-5.1
ENSOCUG00000010814	Malic enzyme 1(ME1)	-5.566
ENSOCUG00000021126	Metallothionein-2A(LOC100343299)	-5.754

*Ratio represents the fold change (vitrified-transferred/naturally conceived).

1069

1070 **Table 4. Functional analysis of the differentially expressed transcripts.**

Category*	Term	Count	p-value
BP	Cellular response to zinc ion	3	9.40E-04
BP	Negative regulation of growth	3	2.00E-03
BP	Antigen processing and presentation of exogenous peptide antigen via MHC class II	2	4.00E-02
BP	Erythrocyte homeostasis	2	4.70E-02
BP	Apoptotic cell clearance	2	6.60E-02
BP	Immune response	4	6.60E-02
CC	Extracellular space	12	1.20E-03
CC	MHC class II protein complex	3	1.80E-03
CC	Perinuclear region of cytoplasm	7	6.80E-03
CC	Extracellular matrix	4	1.00E-02
CC	Nucleus	17	3.00E-02
CC	Low-density lipoprotein particle	2	3.50E-02
CC	Extracellular exosome	17	8.80E-02
CC	Cytoskeleton	3	9.00E-02
MF	Peptide antigen binding	3	1.20E-03
MF	Oxidoreductase activity, acting on paired donors, with oxidation of a pair of donors resulting in the reduction of molecular oxygen to 2 molecules of water	2	1.80E-02
MF	Scavenger receptor activity	3	1.80E-02

KEGG	Antigen processing and presentation	5	1.00E-03
KEGG	Biosynthesis of unsaturated fatty acids	4	1.30E-03
KEGG	Mineral absorption	4	3.20E-03
KEGG	Staphylococcus aureus infection	4	4.60E-03
KEGG	Toxoplasmosis	5	1.20E-02
KEGG	Asthma	3	1.50E-02
KEGG	Phagosome	5	2.00E-02
KEGG	MAPK signalling pathway	6	2.50E-02
KEGG	Influenza A	5	2.70E-02
KEGG	Graft-versus-host disease	3	2.70E-02
KEGG	HTLV-I infection	6	3.10E-02
KEGG	Allograft rejection	3	3.40E-02
KEGG	Amoebiasis	4	3.70E-02
KEGG	Type I diabetes mellitus	3	4.50E-02
KEGG	Autoimmune thyroid disease	3	5.00E-02
KEGG	Intestinal immune network for iga production	3	5.10E-02
KEGG	Fatty acid metabolism	3	5.50E-02
KEGG	Systemic lupus erythematosus	4	6.60E-02
KEGG	Drug metabolism - other enzymes	3	7.30E-02
KEGG	Inflammatory bowel disease (IBD)	3	7.70E-02
KEGG	Viral myocarditis	3	8.30E-02
KEGG	Leishmaniasis	3	9.30E-02

*Functional analysis of the differentially expressed transcripts was referred to the GO term annotation according to the biological process (BP), cellular component (CC) and molecular function (MF) classification, and the KEGG pathways in which they are involved.

1077 **Table 5. Differentially expressed proteins in liver tissue.**

Uniprot accession	Gene name	Ratio*
G1SE36	Hexose-6-phosphate dehydrogenase/glucose 1-dehydrogenase	2.206
G1T489	Acid phosphatase 1, soluble	2.167
G1TWY4	N-acetyl-alpha-glucosaminidase	1.639
G1T103	Chromosome 4 open reading frame, human c12orf10	1.174
G1U6H4	Dimethylarginine dimethylaminohydrolase 2	0.991
P33047	Apolipoprotein C1	0.8
P35748	Myosin heavy chain 11	0.732
G1SHK6	Heterochromatin protein 1 binding protein 3	0.715
G1TH06	RAN binding protein 1	0.615
G1SSL0	Endoplasmic reticulum protein 29	0.614
G1U7D9	Solute carrier family 27 member 5	0.568
G1SR13	Stomatin like 2	0.559
G1U6B2	Aminolevulinate dehydratase	0.4
Q08863	Glutathione S-transferase alpha I	0.272
G1T6G8	Dimethylglycine dehydrogenase	0.258
G1SV12	Acyl-coa dehydrogenase, C-2 to C-3 short chain	0.127
G1T9N2	ATP synthase, H+ transporting, mitochondrial Fo complex subunit D	-0.222
G1U758	Keratin 18	-0.318
G1T3R1	Glutaredoxin 5	-0.323
G1U7C5	Ribosome binding protein 1	-0.324
P53787	Elongation factor 1 delta	-0.341

G1U430	TATA-box binding protein associated factor 15	-0.363
G1SST9	RAD23 homolog B, nucleotide excision repair protein	-0.365
G1SYL8	Transcription elongation factor B subunit 2	-0.401
G1SJ56	Vinculin	-0.408
G1T5E6	Sorting nexin 2	-0.457
G1T3V0	High density lipoprotein binding protein	-0.464
G1SRX2	Elongation factor Tu GTP binding domain containing 2	-0.479
G1TAP1	Pyrophosphatase	-0.494
G1SDQ1	Arsenite methyltransferase	-0.521
G1T0V1	Tumour protein p53 inducible protein 3	-0.524
G1TUD6	Proteasome 26S subunit, ATPase 4	-0.539
G1SFR8	Ribosomal protein S12	-0.563
O97972	Indolethylamine N-methyltransferase	-0.579
B7NZG7	Sorting nexin 3	-0.605
G1T0Y9	Dynactin subunit 2	-0.61
G1STH0	Splicing factor 3a subunit 1	-0.617
G1SYV0	Proteasome 26S subunit, ATPase 2	-0.619
G1T7G4	Growth arrest specific 2	-0.623
G1SZ85	3'(2'), 5'-bisphosphate nucleotidase 1	-0.647
G1TIR9	UDP-glucuronosyltransferase 2B31	-0.662
G1TWL2	Golgin subfamily A member 2	-0.666
G1SIT9	Tyrosine 3-monooxygenase/tryptophan 5-monooxygenase activation protein beta	-0.689
G1SDJ3	Up-regulated during skeletal muscle growth 5 homolog	-0.731
G1SCF7	Plakophilin 2	-0.737

G1SUS6	Secretion associated RAS related GTPase 1B	-0.749
G1SYG1	Arylformamidase	-0.764
G1TA37	Barrier to autointegration factor 1	-0.796
G1TPN3	Heterogeneous nuclear ribonucleoprotein A/B	-0.834
U3KM96	RAP1B, member of RAS oncogene family	-0.856
G1SKS9	Thioredoxin reductase 1	-0.879
B7NZQ6	GDP dissociation inhibitor 1	-0.912
G1T286	VPS29, retromer complex component	-0.916
G1TBS2	Ruvb like AAA ATPase 1	-0.952
G1SL53	TBC1 domain family member 9B	-0.993
G1SYD2	Adenylate kinase 4	-1.024
G1T9T6	Ethanolamine-phosphate phospho-lyase	-1.033
G1STF9	Eukaryotic translation initiation factor 3 subunit I	-1.051
G1TTU6	S-phase kinase associated protein 1	-1.118
G1TEI2	Ferredoxin 1	-1.134
G1TX53	NADH:ubiquinone oxidoreductase subunit A8	-1.174
G1SIZ2	Ribosomal protein S20	-1.209
G1SCP7	IQ motif containing gtpase activating protein 1	-1.226
G1U826	ATPase H+ transporting V1 subunit G1	-1.245
Q29508	Cytochrome P450 2E1	-1.247
G1SR28	Platelet activating factor acetyl hydrolase 1b catalytic subunit 3	-1.358
G1TBN0	Cold shock domain containing E1	-1.375
G1THD9	Cytochrome P450 3A6	-1.397
G1SV10	Wiskott-Aldrich syndrome like	-1.401
G1SFE9	Activator of Hsp90 ATPase activity 1	-1.56

G1SVD5	Adenosine deaminase, RNA specific	-1.588
G1SPL1	Phosphoglycerate dehydrogenase	-1.597
G1SSR3	Lon peptidase 2, peroxisomal	-1.648
O79431	ATP synthase F0 subunit 8	-1.793
G1SEH7	NADH:ubiquinone oxidoreductase subunit B8	-1.875
G1SCT0	Cytoskeleton associated protein 4	-2.016

*Ratio represents the fold change (vitrified-transferred/naturally conceived).

Table 6. Functional analysis of differential expressed proteins.

Category*	Term	Count	P-Value
BP	Glycine metabolic process	2	2.80E-02
BP	Protein transport	3	4.40E-02
BP	Response to bacterium	2	6.10E-02
BP	Osteoblast differentiation	3	6.20E-02
BP	ATP synthesis coupled proton transport	2	8.80E-02
CC	Extracellular exosome	32	3.80E-09
CC	Membrane	11	4.20E-03
CC	Cytosol	9	2.20E-02
CC	Mitochondrial proton-transporting ATP synthase complex, coupling factor F(o)	2	3.80E-02
CC	Retromer complex	2	6.90E-02
MF	Poly(A) RNA binding	11	1.20E-02
MF	Electron carrier activity	3	1.60E-02
MF	ATPase activity	3	6.60E-02
MF	Oxidoreductase activity, acting on paired donors, with incorporation or reduction of molecular oxygen, reduced flavin or flavoprotein as one donor, and incorporation of one atom of oxygen	2	9.60E-02

KEGG	Metabolic pathways	20	1.60E-03
KEGG	Oxidative phosphorylation	6	3.40E-03
KEGG	Protein processing in endoplasmic reticulum	6	9.20E-03
KEGG	Chemical carcinogenesis	4	4.20E-02
KEGG	Huntington's disease	5	6.10E-02

*Functional analysis was referred to the GO term annotation according to the biological process (BP), cellular component (CC) and molecular function (MF) classification, and the KEGG pathways in which they are involved.

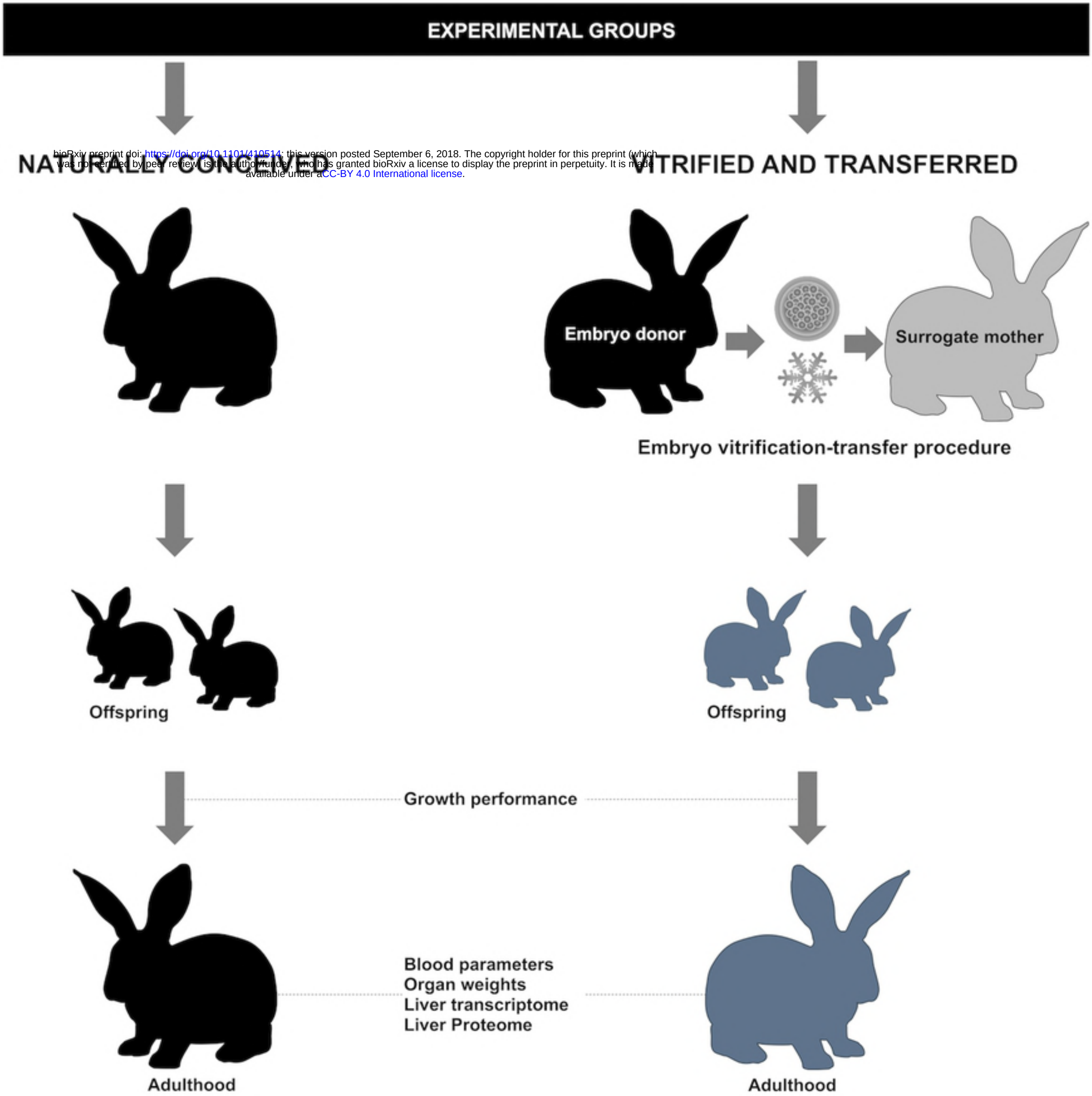

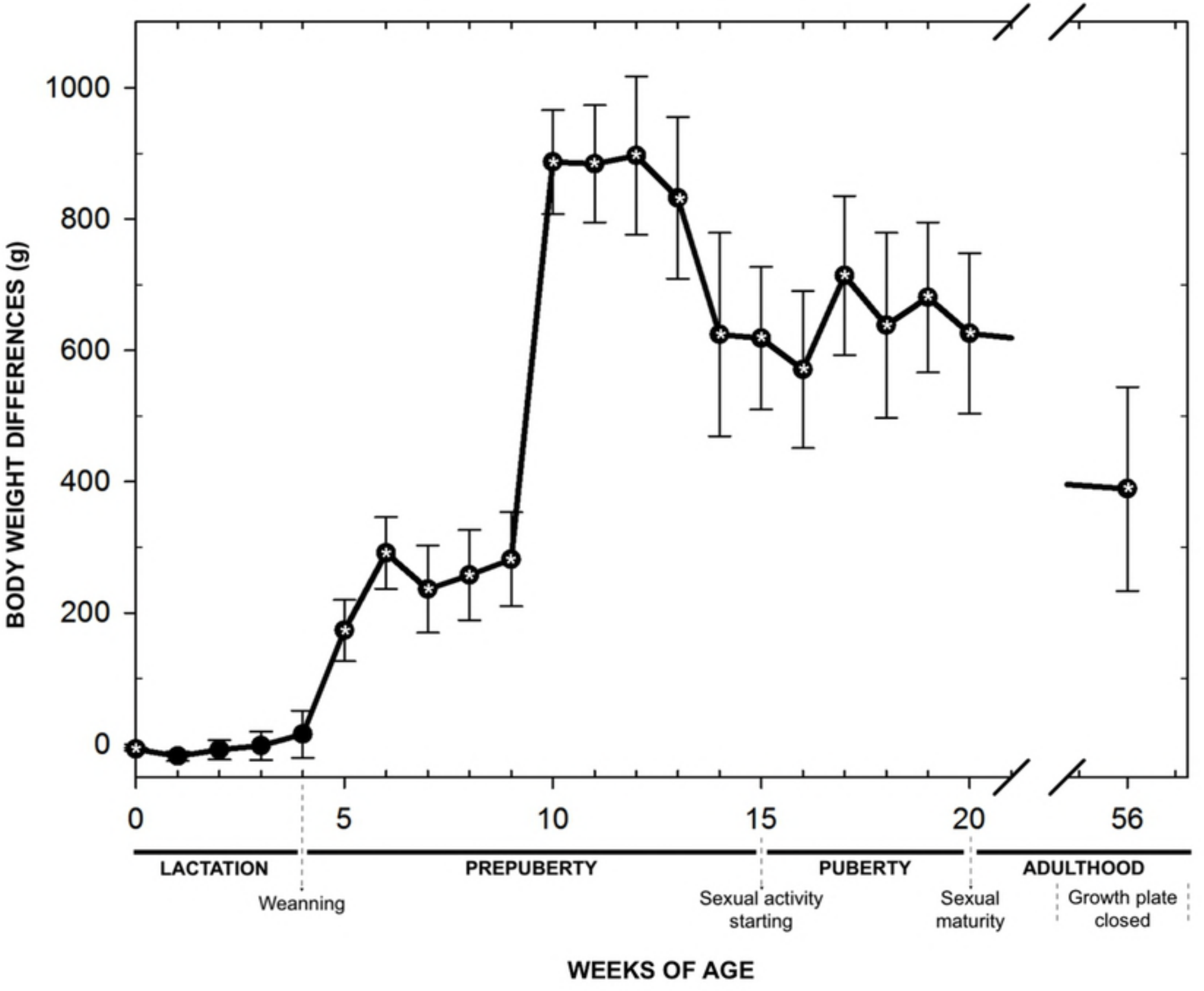
BODY WEIGHT DIFFERENCES (g)
1000
800
600
400
200
0
0
5
10
15
20
56
LACTATION
PREPUBERTY
PUBERTY
ADULTHOOD
Weanning
Sexual activity starting
Sexual maturity
Growth plate closed
WEEKS OF AGE

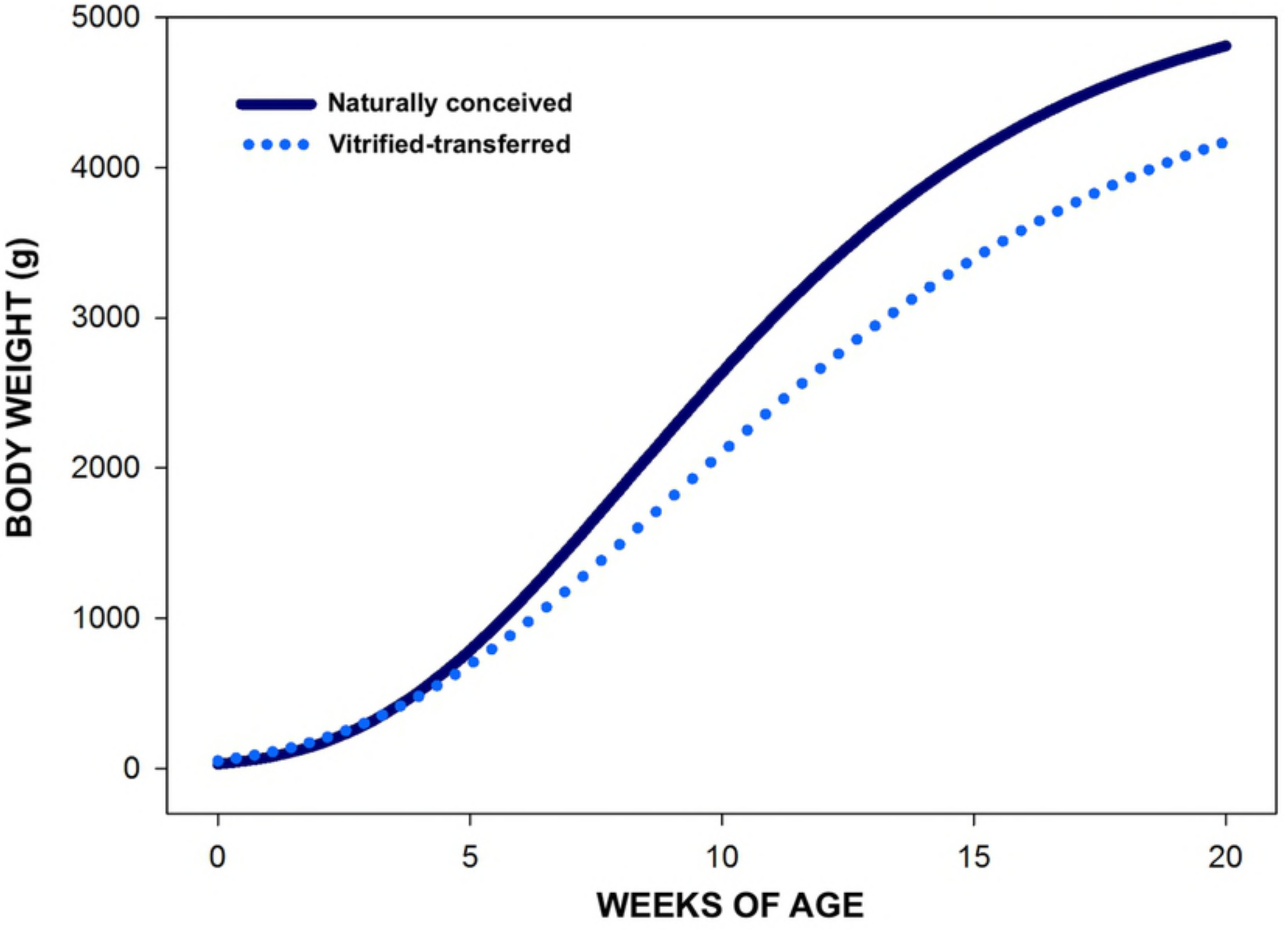
Naturally conceived
Vitrified-transferred
BODY WEIGHT (g)
5000
4000
3000
2000
1000
0
0
5
10
15
20
WEEKS OF AGE

A

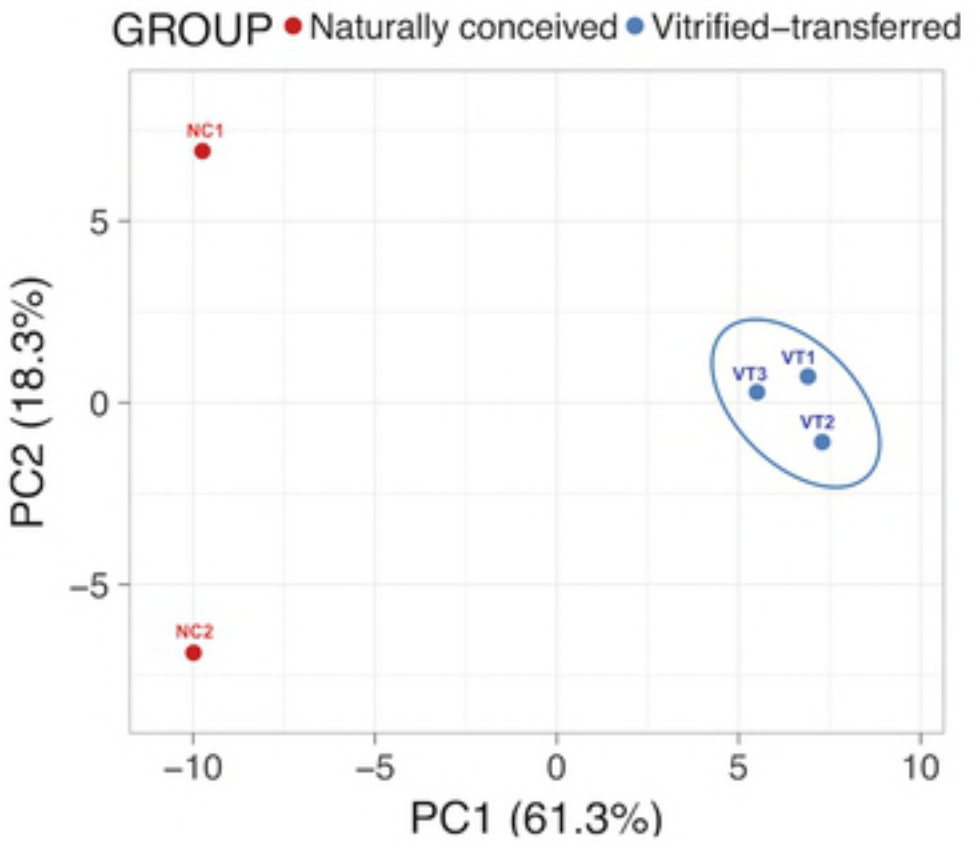

B

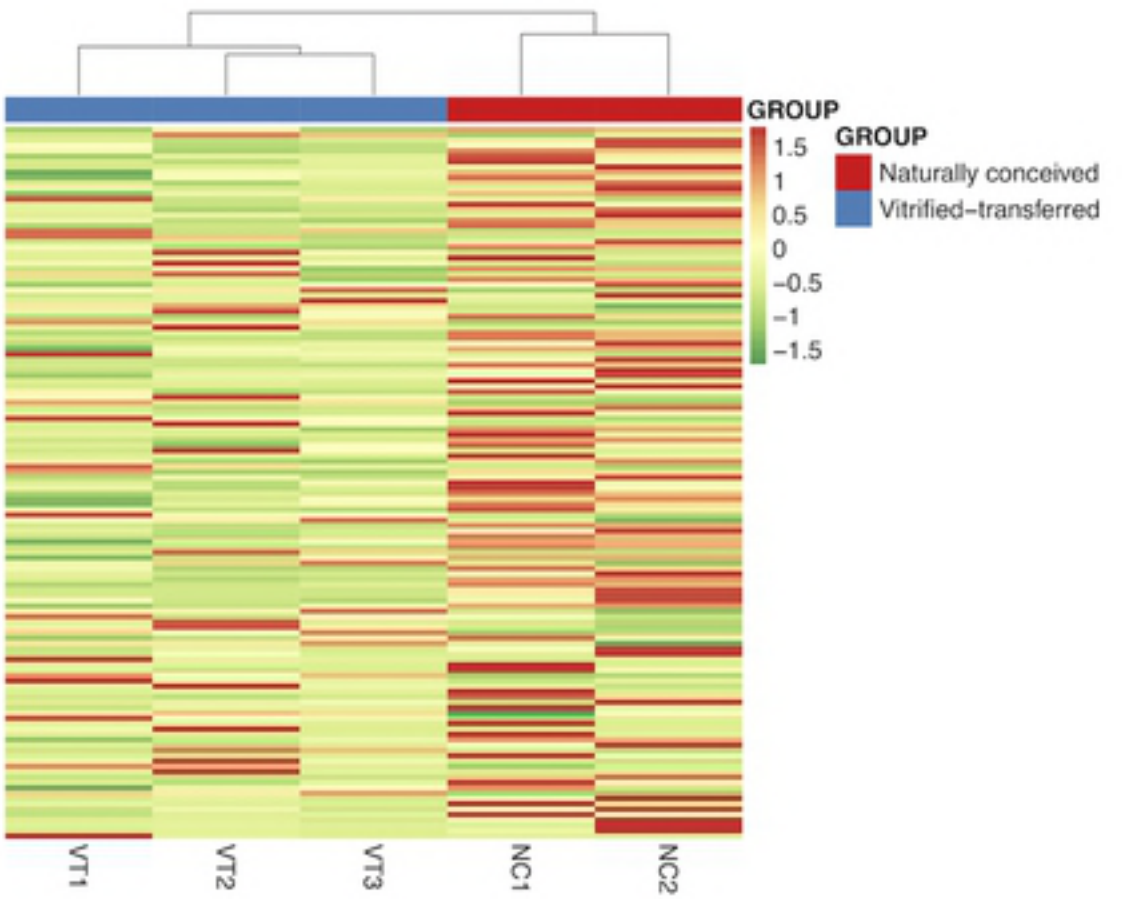

C

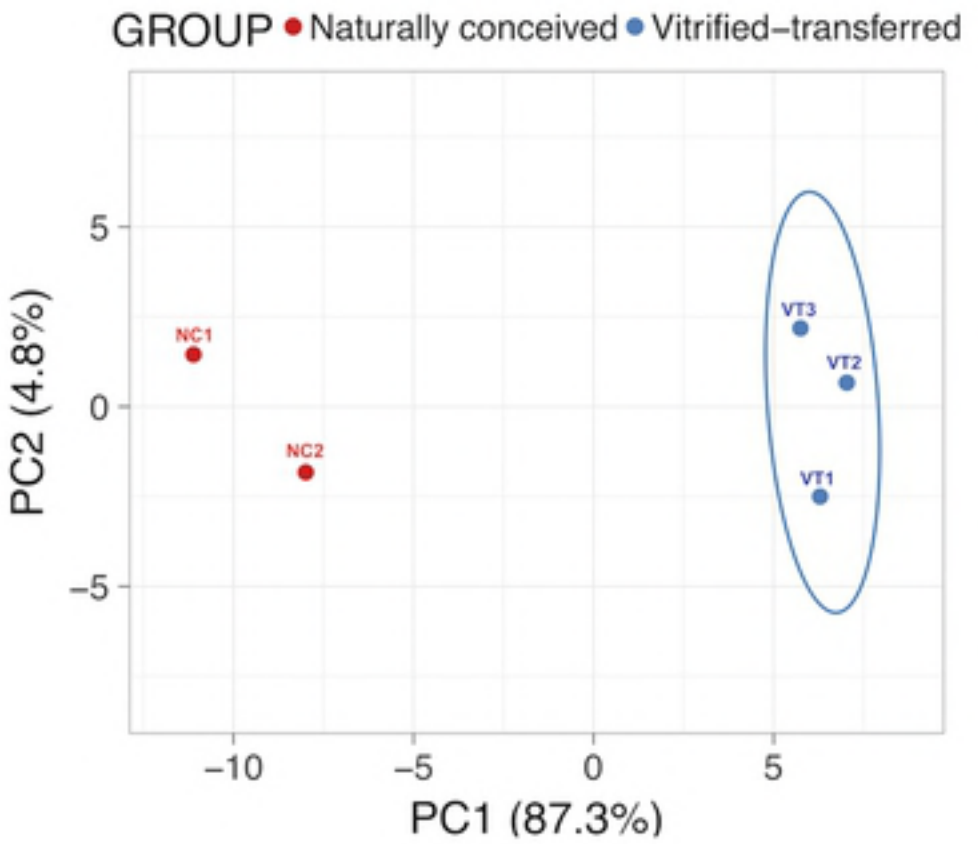

D